B.S.Bal'zhinimaev
Russ. Chem. Rev., 2020, **89** (11) 1184 – 1203

https://doi.org/10.1070/RCR4958

Catalysis by platinum and palladium species confined in the bulk of glass fibre materials

Bair S. Bal'zhinimaev

Boreskov Institute of Catalysis, Siberian Branch of the Russian Academy of Sciences, prosp. Akademika Lavrent'eva 5, 630090 Novosibisk, Russian Federation

The results of studies on the application of silicate glass fibre materials in catalysis are summarized and analyzed. Despite the very low noble metal content, catalysts based on these materials showed exceptionally high activities and selectivities in some catalytic reactions. This is due to specificity of the glassy state, which makes it possible, first, to confine highly dispersed palladium and platinum species in the bulk of glass fibres and, second, selectively absorb polar molecules, thus excluding the undesirable reactions involving non-polar molecules. The size dependences of the complete oxidation of propane and selective hydrogenation of acetylene, the nature of the structure sensitivity of these reactions and the reaction mechanisms are discussed. Ways for improving glass fibre catalyst performance are proposed and examples of the successful application of Pt/glass fibre catalysts for purification of industrial gases from volatile organic compounds are given.
The bibliography includes 175 references.

Contents

1. Introduction 1184
2. Structure and physicochemical properties of silicate glass 1186
3. Modification of glass fibres with organic nitrogen bases 1188
4. Synthesis and properties of the Pd(Pt)/glass fibre catalysts 1189
5. Selective hydrogenation of acetylene with Pd/glass fibre catalysts 1190
6. Complete oxidation of hydrocarbons on the Pt/glass fibre catalysts 1194
7. Oxidative degradation of organochlorine compounds on the Pt/glass fibre catalysts 1198
8. Conclusion 1199

1. Introduction

Simple silicate glasses, containing group 1, 2 and 3 metal oxides apart from silicon dioxide, have been known for a long time; they are produced on a large scale and are widely used for the manufacture of windows, lenses, bottles and containers and in architecture and art. Depending on the chemical composition and application area, glass materials are produced as large and small sheets, micro- and macrospheres, glass cotton, fibres and threads of various diameters and textures. The scope of applicability of these materials can be markedly expanded by leaching, *i.e.*, replacing the alkali or alkaline earth metal ions by protons or by larger potassium ions *via* ion exchange reactions with solutions of inorganic acids or bases. In the former case, glasses are widely used, after high-temperature treatment, as heat and electric insulating materials. An increase in the ionic radius of the alkali metal leads to increasing compressive forces, which toughens the glass surface and prevents crack propagation. These glasses are successfully used in electronics and biomedicine, in particular, for the manufacture of injection ampoules, smartphones, laptops, *etc*.[1]

Apart from the above traditional applications, glass materials as microfibres and fabric blends made of them have started to be used in catalysis. These materials are chemically inert and have lower hydraulic resistance and better mass transfer than granulated catalysts; also, they can be formed as flexible structured catalyst layers of virtually any shape.[2–4] Finally, this can lead to new designs of catalytic reactors.

The first glass fibre (GF) catalysts appeared approximately 40 years ago when platinum metal was deposited on the surface of borosilicate glass fibres.[5] These catalysts showed higher activity in the treatment of vehicle exhaust gases to remove carbon monoxide and hydrocarbons than the conventionally used catalytic systems. For increasing the activity, the fibres were leached by hydrochloric acid to form porous glass fibres due to removal of boron and sodium compounds from the glass. In this case, Pt(Pd)/GF catalysts showed a higher activity towards carbon monoxide and toluene oxidation reactions than their analogues prepared from non-porous silicate fibres.[6] As the content of the noble metal increased (up to 1 mass %), the activity increased, with the platinum catalyst being much superior over the palladium one. However, the borosilicate fibres proved to be unstable and were mechanically damaged during the gas-phase reactions. Therefore, more stable non-porous glasses are used more often in heterogeneous catalysis. Nevertheless, porous glasses with 1 nm to 1 μm pore size, including systems with a hierarchical porous structure, were developed on the basis of borosilicates.[7]

B.S.Bal'zhinimaev. Doctor of Chemical Sciences, Chief Researcher, Head of the Laboratory of New Materials Testing in Catalysis at the BIC SB RAS.
E-mail: balzh@catalysis.ru
Current research interests: kinetics and mechanisms of heterogeneous catalytic reactions; selective oxidation and hydrogenation of hydrocarbons; ethylene and propylene epoxidation; synthesis of light alkenes from paraffins; the use of new materials in heterogeneous catalysis, in particular, glass fibre catalysts.

Translation: S.P.Svitanko

Received 12 April 2020

© 2020 Uspekhi Khimii, ZIOC RAS, Russian Academy of Sciences and IOP Publishing Limited

These glasses are widely utilized as membranes and sensors,[8] reference samples for texture measurement,[9] and for studying diffusion processes in porous solids.[10] In addition, porous borosilicate materials, together with other types of silicate glass, often serve as supports for TiO_2-based photocatalysts for the degradation of toxic organic and organochlorine compounds.[11 – 18]

In order to increase the surface area, the glass fibre materials were coated by a thin film of titania (zirconia) or alumina, which were then coated by noble metals. These composite catalysts actually exhibited higher activities in the oxidation of propane. In the reaction catalyzed by $Pt/TiO_2/GF$, a 100% conversion of propane was attained in a very short contact time ($\sim$0.1 s).[19] The main drawback of these catalysts is peeling off of titania upon mechanical and thermal impact. Nevertheless, modification of weakly hydrophobic silicate glasses with silicon compounds considerably increased the binding strength between the titania and the glass fibre and the uniformity of deposition.[20] Testing of these composite catalysts in n-heptane oxidation showed that at low temperature, n-heptane was mainly oxidized to C_3-C_4 ketones, while at high temperature, the oxidation gave CO_2 and alkenes.[20, 21]

Promising results were obtained in the testing of Pt/GF catalysts in the oxidation of SO_2.[4, 22, 23] These catalysts showed high potential for the treatment of sulfur dioxide-rich gases, because, unlike the vanadium sulfuric acid catalysts, they retained activity at high temperatures.[22, 23] In addition, Pt/GF catalysts proved to be active towards the selective reduction of nitrogen oxides;[24] in the presence of excess oxygen, the deNOx process scarcely took place. The kinetic features of carbon monoxide and propane oxidation catalyzed by glass fibres or by conventional catalysts were similar, including self-oscillations of the CO reaction rate.[25] However, the activities of glass fibre and conventional catalysts in the complete oxidation of hydrocarbons,[5, 19, 26] CO [6, 25, 27] and SO_2 were not properly compared, because the specific rates of reactions and turnover frequencies (TOFs) were not measured.

Apart from metal particles, transition metal oxides and oxide mixtures were also deposited on the glass fibres. In particular, the Cu^+-Cu^0 clusters deposited on glass fibres exhibited high activity and selectivity in the liquid-phase oxidation of cyclohexane to cyclohexanol and cyclohexanone.[28] Mixed copper(I) and copper(II) oxides showed a reasonably good activity towards the complete oxidation of isopropyl alcohol,[29] although above 250 °C, irreversible deactivation of the catalyst started, apparently due to undesirable phase transformations. A relatively high activity towards CO oxidation was found for supported Co – Cu – Ce oxide nanoparticles;[30] however, they were markedly less active than platinum catalysts.

In addition to gas-phase reactions, GF catalysts were also employed in liquid-phase processes such as hydrogenation of phenylacetylene [31] and nitrobenzene,[32] water purification from methylene blue dye at different pH values [33] and reduction of nitrite and nitrate anions to molecular nitrogen in a water denitrification process.[34, 35] Despite the obvious technological advantages of glass fabric catalysts over finely dispersed powders for suspension processes, the problem of loss of noble metals during the process is still relevant. This probably holds up the design of industrial liquid-phase processes based on GF catalysts.[34] In almost all of the above examples, glass fibres are used as differently woven fabric of various geometry, which allows the design of structured catalyst beds with good hydrodynamic characteristics.[3, 4] Glass fibre-based glass wool is used much more rarely, although in this case, too, the surface can be decorated with various metals. Glass wool-based catalysts were successfully tested in the hydrogenation of nitrobenzene to aniline, C – C bond formation reaction, N – C cycloaddition and so on.[36]

Glass fibre catalysts are prepared using the same approaches that are applied to obtain conventional catalytic systems. Most often, this is done by impregnation and adsorption from precursor solutions and subsequent reduction to the metallic state. Therefore, active metal particles are located on the outer surface of the fibres. A special place is occupied by studies in which metal (mainly Pt and Pd) precursors are introduced into the bulk of glass fibres by ion exchange reactions, instead of being deposited on the surface. In this case, the content of platinum metals in the catalyst decreases by more than an order of magnitude to reach extremely low values of $\sim$0.01% – 0.02%. This sharp decrease in the content of noble metals alone is beneficial for the competitive potential of GF catalysts. The location of the Pt active sites in the bulk does not restrict the catalytic reaction rate, because the reactant diffusion is markedly faster in the bulk of glass.[37] Furthermore, Pt/GF catalysts demonstrated much higher activity towards complete oxidation of hydrocarbons (propane and butane).[22] The reaction rate per unit area of the metal surface was several tens of times higher than that for supported catalysts. Similarly, Pd particles located in the bulk of glass proved to be more selective in acetylene hydrogenation than palladium particles supported on usual materials.[38]

The surface area of glass fibres can be significantly increased by surface modification with an organic nitrogen base and formation of a film of a porous silicate phase.[39] In this case, the GF specific surface area and the rate of complete oxidation of propane considerably increased.[39, 40] The rate of selective hydrogenation of acetylene also increased, while the selectivity of the Pd/GF catalyst for the complete conversion of acetylene was even higher than that of the modern bimetallic catalyst.[41] It should be noted that, unlike the TiO_2/GF or TiO_2-SiO_2/GF composites mentioned above, the porous film was attached much more strongly to the glass fibre and was not detached.

Over the last decade, two reviews were published,[3, 4] summarizing the existing results (mainly empirical) on the use of glass fibre materials in catalysis. One review [3] presents particular examples of application of structured materials in catalysis, covering not only glass, but also ceramic and metallic fibres. Although a comprehensive account of benefits of GF catalysts for various reactions is presented, the attention is focused on the technological advantages, in particular, hydrodynamic properties, which ensure effective mass and heat transfer in the structured beds in chemical reactors. The other review [4] gives examples of practical application of GF catalysts in particular processes such as nitric and sulfuric acid production, removal of volatile organic compounds (VOCs) and so on. However, the fundamental causes for the differences between the activity and selectivity of the conventional and GF catalysts remain obscure, which precludes the possibility of evaluating the potential of these materials in catalysis and finding more efficient applications.

The present review is devoted to identification of the key physicochemical characteristics of silicate glasses that are responsible for their unusual catalytic behaviour. First of

all, this is the ability of glass fibres to confine metal and metal–oxide clusters, which have high activity and selectivity in complete oxidation of hydrocarbons and hydrogenation of acetylene. Second, this is the ability of GFs to selectively absorb (dissolve) only polar molecules, which suppresses undesirable reactions. Ways for increasing the activity and selectivity of GF catalysts are proposed on the basis of analysis of the size dependences of TOF for these reactions, the nature of structure sensitivity and the reaction mechanisms. Examples of successful operation of Pt/GF catalysts in the treatment of industrial gases for removal of VOCs are given in the Conclusion.

The following designations and acronyms are used:

C — concentration,

$^*C_i$ — concentration of carbon-labelled ith hydrocarbon,

Cl-VOCs — chlorinated volatile organic compounds,

D — diffusion coefficient,

d — particle size,

GF — glass fibre,

h — depth of location of the active sites,

P — pressure,

Pt_S and Pd_S — platinum and palladium atoms located on the surface,

Pt_V and Pd_V — platinum and palladium atoms located in the bulk,

S — selectivity of the reaction,

SEM — scanning electron microscopy,

SSITKA — steady state isotopic transient kinetic analysis,

T — temperature,

τ — diffusion time,

1,2,3,4-TeCDD — 1,2,3,4-tetrachlorodibenzo-1,4-dioxin,

TMA — tetramethylammonium cation,

TOF — turnover frequency,

TPD — temperature programmed desorption,

VOCs — volatile organic compounds,

XPS — X-ray photoelectron spectroscopy.

2. Structure and physicochemical properties of silicate glass

Glass occupies an intermediate position between the solid and liquid states of matter, with transition from one state to another being gradual rather than stepwise as in phase transitions. The physicochemical properties such as viscosity, heat and electrical conductivity change continuously rather than stepwise. From the thermodynamic standpoint, glass is a metastable phase with a local minimum of the internal energy at a highly extended phase transition. In this respect, glassy state resembles a supercooled, but a highly viscous liquid.

Although glasses have been known for a very long time, data on their molecular structures are mainly empirical.[42] The structure of simplest sodium silicate glasses was represented as a system of randomly linked chains of SiO_4 tetrahedra the vertices of which are connected *via* oxygen atoms, while the Na^+ cations surrounded, on average, by six oxygen atoms are uniformly distributed in various voids. Later, EXAFS† studies demonstrated that alkali metal cations are actually ordered (segregated) and occur in microcavities, which separate the dense areas consisting of silicon–oxygen tetrahedra.[43] In essence, this was a layered structure composed of alternating areas of SiO_4 and charge-balancing alkali or alkaline earth metal cations. The size of SiO_4 areas in Na silicate glasses was determined by NMR and IR spectroscopy; also, it was demonstrated that sodium cations are actually incorporated into the silicon–oxygen framework *via* terminal (non-bridging) oxygen atoms bound to silicon.[44] Under the action of mineral acids, glass leaching takes place, that is, the replacement of sodium cations by protons. The silica framework remains invariable, because siloxane bonds are not cleaved; hydrogen-bonded hydroxyl groups are formed in microcavities.[44] As this takes place, glass loses considerable mass, so that the density of silicate glass fibre ($\sim$2.2 g cm^{-3}) is substantially lower than the density of crystalline SiO_2 (2.65 g cm^{-3}).

The external appearance of leached glass fabric manufactured by the Research and Production Association Stekloplastik, which was used to manufacture catalysts, is shown in Fig. 1 *a*. The silicate glass fabric is woven of threads 1 mm in diameter, composed of elementary fibres 6–7 μm in diameter (Fig. 1 *b*). The structure of glass fibres is layered and represents 3–4 rows of SiO_4 tetrahedra (dense area), which are randomly connected by oxygen bridges; these rows alternate with low-density areas accommodating OH groups. As an example, Fig. 2 presents the molecular structure of the leached Al silicate glass fibre.[44] The proposed structure explains well the experimental ratio of 45 : 55 between the ^{3}Q and ^{4}Q tetrahedra, which contain three and four bridging oxygen atoms, respectively. In other words, the number of SiO_4 tetrahedra with a hydroxyl group is commensurable with the number of tetrahedra in which the silicon atom is surrounded by only bridging oxygen atoms. An approximately the same ratio between the ^{3}Q (surface silanols) and ^{4}Q structures is observed in the case of silica gel with a specific surface area of $\sim$700 m^2 g^{-1}. The Al^{3+} cations ($\sim$1.5 at.%) isomorphously substitute Si^{4+}, and the charge is balanced *via* the formation of Si–OH–Al bridging hydroxyl groups with acidity similar to that of zeolites.[45,46]

Apart from silicon, not only aluminium, but also zirconium or lanthanides of the La–Ce family can be used as the second structuring elements. Unlike the Al silicate GF, the Zr silicate GF has a framework rather than a layered structure.[47–49] The framework is formed by six-coordinate Zr^{4+} cations connected by two to four SiO_4 tetrahedra.[47] This framework structure ensures a high thermal stability of zirconium glass fibres (up to 1200 °C); hence, they can be used as supports for the preparation of catalysts for complete oxidation of VOCs. In these processes, great overheating of the catalyst bed is possible because of variation of VOC concentrations. Palladium catalysts active

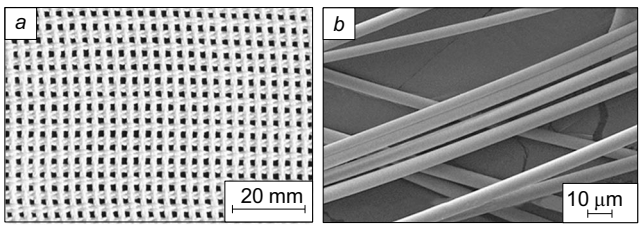


Figure 1. External appearance of silicate glass fabric (*a*) and elementary fibres according to scanning electron microscopy (SEM) data (*b*).[40]

† Extended X-ray absorption fine structure.

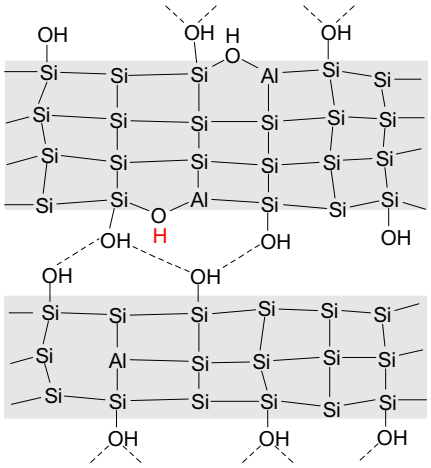


Figure 2. Molecular structure of the leached Al silicate glass fibre. For simplicity, the SiO_4 and AlO_4 tetrahedra are designated by Si and Al, respectively.[44]

for the selective hydrogenation of acetylene are manufactured using Al silicate glass fibres.

The size of loose areas accommodating OH groups and molecular water can be indirectly estimated by IR spectroscopy. The spectra of annealed Zr, Al and La – Ce silicate GFs exhibit narrow bands for isolated bridging OH groups, which are considerably shifted to low frequency region.[50] By analogy with zeolites, it can be considered that the position of these bands depends on the size of channels: the smaller the size, the lower the frequency. In this case, the smallest microcavity size is inherent in Zr silicate glass, while the La – Ce silicate glass has the largest microcavities. In the former case, the absorption band for the bridging OH groups was located closely to the band for isolated hydroxyl groups in ZSM-5, while in the latter case, it was close to the band of the same groups in Y zeolite, *i.e.*, the cavity sizes in the Zr and La – Ce silicate GFs correspond to the size of channels in the ZSM-5 (0.56 nm) and Y (1.1 nm) zeolites, respectively. The Al silicate glass fibres occupy an intermediate position regarding the microcavity diameter. It is noteworthy that the size of cavities in the zirconium glass estimated by NMR spectroscopy was markedly greater (up to 2 nm).[49]

The total content of silanol groups in glass fibres is 5% – 6%; they retain up to ~2.5% of molecular water by means of hydrogen bonds.[44] Water is fairly corrosive towards silicate glasses, because it induces cleavage of the siloxane bonds in the dense phase to give Si – OH and/or Al – OH groups.[51 – 53] The amount of molecular water is determined by equilibrium between the hydrolysis of bridging bonds and dehydration of the resulting OH groups. Therefore, during the temperature programmed desorption (TPD), first, molecular water is released and then, at higher temperatures, activated dehydroxylation of H-bonded hydroxyl groups takes place.[44, 54] This process is reversible and, on contact with a moist medium, water again diffuses into the glass fibre and hydrolyzes the Si – O – Si or Al – O – Si bridging bonds, thus restoring the equilibrium concentrations of hydroxyl groups and molecular water. However, high-temperature annealing of some glasses may give rise to irreversible phenomena. Upon annealing in dry air at temperatures of >800 °C, the Al silicate glass is completely and irreversibly dehydroxylated, which induces crystallization and mechanical destruction.[23, 44] More thermally stable Zr silicate glasses have a framework rather than a layered structure;[47] however, the TPD of water from these and above-considered glasses is qualitatively the same.

In terms of physical properties, glass more closely resembles liquids than solids; therefore, diffusion in glass is much faster. The mobility of water in leached Zr silicate glass fibres was estimated at room temperature from the time dependence of the H – D exchange rate measured by IR spectroscopy.[55] Then the diffusion coefficient of water molecules was calculated to be 10^{-11} cm^2 s^{-1} using Fick's law; this value is several orders of magnitude larger than the value characteristic of solid. The water diffusion coefficient at 400 °C was estimated by steady state isotopic transient kinetic analysis (SSITKA) using $H_2{}^{18}O$, which resulted in the value of 2×10^{-8} cm^2 s^{-1} (Refs 37 and 56). The diffusion of water in unleached Na silicate glasses was also studied by IR spectroscopy by measuring the concentration of hydroxyl groups formed upon the hydrolysis of the O – Na bonds.[57, 58] The estimated water diffusion coefficient at ~400 °C was $10^{-10} - 10^{-11}$ cm^2 s^{-1}, which is approximately three orders of magnitude lower than that for the leached glass. It is assumed that so pronounced differences in the mobility of water are due to different mechanisms of water transfer: the diffusion of water in the Na silicate glass occurs *via* hydrolysis – dehydration chemical reactions,[51, 59] while in the leached glass, water molecules migrate *via* the interaction with hydroxyl groups by the relay mechanism.[55, 56] It is clear that in the latter case, diffusion is much faster due to weaker hydrogen bonds. However, in zirconium GFs annealed at high temperature, the diffusion of water is substantially retarded, because the concentration of hydroxyl groups decreases to a very low level.[55]

Glass fibres efficiently absorb NH_3 at elevated temperature as a result of a reversible reaction of the ammonium ions with protons[50] and also absorb acetylene.[54, 60] According to UV spectroscopy data, the colour of glass fibres changed from white to yellow and yellow-brown with increasing temperature, which was interpreted as the formation of first short $-(-CH{=}CH-)_m-$ and then longer oligomers containing 6 – 8 conjugated double bonds.[61] In other words, rather extended acetylene structures are formed in the glass fibre bulk. Since the Al silicate glass is layered, oligomers are presumably linear rather than cyclic. It is noteworthy that the spectrum exhibits a broadened signal (compared to that of acetylene gas), which can be assigned to acetylene molecules confined in a narrow space, apparently, in equilibrium with acetylene oligomers. The Pd/GF catalyst can absorb up to 0.14 mass % acetylene or, considering the formation of oligomers, up to 0.5 mass %.[38, 54] Meanwhile, glass fibres absolutely do not absorb ethylene or ethane, despite their high concentrations and high pressures in the gas phase.

A particularly interesting issue is how the non-polar hydrogen molecule can be absorbed. Direct measurements demonstrated that hydrogen is not absorbed by either the support or the catalyst. However, during the reaction, *i.e.*, in the presence of $H_2 + C_2H_2$, both acetylene and hydrogen are absorbed. The absorbed hydrogen is released at high temperature (250 – 450 °C) and the amount of this hydrogen is 1.5 – 2 orders of magnitude higher than the number of palladium atoms in the catalyst if the stoichiometry is assumed to be $Pd : H_2 = 1 : 1$.[38, 54] Since H_2 is absorbed only during hydrogenation of acetylene and is released at

high temperature, it can be assumed that hydrogen is strongly bound to the acetylene oligomers $-(-CH=CH-)_m-$. It was shown [62] that the oligomers formed upon acetylene hydrogenation may contain active hydrogen, which participates in the reaction.

Thus, the solubility of gas molecules in glass depends mainly on their electrophysical properties, *e.g.*, dipole moment, polarizability and so on, but not on the size. Polar molecules such as H_2O, NH_3, H_2S (see below) are efficiently absorbed by glass owing to chemical reactions with protons or to hydrogen-bonding to hydroxyl groups. Therefore, the solubility is determined by the heat of absorption and by concentration of molecules. The diffusion coefficient in glass depends primarily on the mechanism of molecular transfer, the structure of the diffusing molecule and functional groups of the environment. The diffusion of water in the leached glass occurs by the relay mechanism, consisting in the transfer of molecular water *via* successive interaction with hydroxyl groups.[57] In the absence of OH groups (or when their concentration is low), the diffusion of H_2O molecules either sharply slows down or does not take place at all.[55]

3. Modification of glass fibres with organic nitrogen bases

Since glass fibres are non-porous, their specific surface area is equal to the geometric one and is < 1 m^2 g^{-1}. This low value can substantially restrict the rate of mass transfer across the gas/glass interface and reduce the absorption capacity of GFs and the catalyst activity. For increasing the specific surface area and mass transfer rate, the glass fibre was coated by a porous oxide layer.[19] This actually increased the catalyst activity, but due to poor adhesion and pronounced difference between the temperature expansion coefficients of glass and the solid oxide, the porous film was readily detached.

The surface of mesoporous silicate materials can be modified by treatment with amines;[63,64] however, in the case of GFs, this did not increase the specific surface area. Then, by analogy with the hydrolysis of silicate glasses, glass fibres were modified by treatment with a strong organic base — tetramethylammonium hydroxide.[39] The key step of this process is the addition of the HO^- anion to the ^{3}Q tetrahedron giving a five-coordinate intermediate, which decomposes to form the $Si-O^-$ residue and hydroxylated silicon species.[51] Long-term (for several days) hydrothermal treatment of GFs markedly changes their surface morphology (Fig. 3): a 70–80 nm-thick film of a new phase appears on the GF surface. This phase results from dissolution–condensation processes of glass components with formation of new siloxane bonds.[65,66] According to modern views,[51,66,67] a gel-like film is actually formed at the glass/solution interface and serves as the diffusion barrier restricting the rate of GF dissolution; therefore, at moderate temperatures, the mass loss of glass fibres is moderate, not exceeding 5%–10%.[39] The new phase proved to be porous with a pore size of 5 nm[39] and a specific surface area of 16 m^2 g^{-1} (these mesopores can be seen in the inset of Fig. 3 as small dark spots on the gel-like film).

For Al silicate GFs, the researchers monitored the dynamics of formation of this phase, starting from the appearance of small roughnesses (nuclei) on the surface, which gradually increased in size until a continuous film

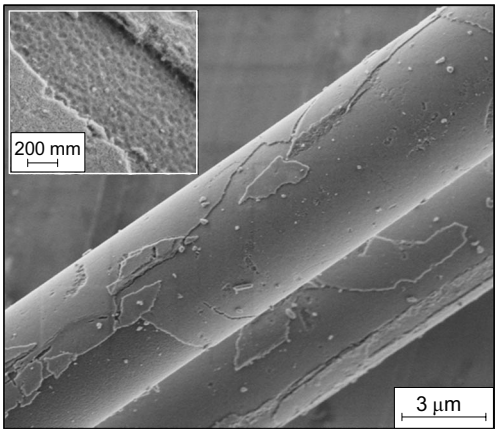


Figure 3. High-resolution SEM image of modified Al silicate glass fibres. The inset shows an enlarged part of the glass fibre surface.[40]

formed. The rate of this process increased with temperature rise, and this dependence was correlated with the increase in the size of glass microcavities accommodating hydroxyl groups. The GF modification proceeded most easily for the relatively loose La–Ce silicate glasses; after hydrothermal treatment under moderate conditions, the specific surface area was as high as 149 m^2 g^{-1}. Zirconium silicate GFs proved to be more stable to alkaline treatment; in this case, a similar film was formed after long-term hydrothermal treatment at high temperature.

According to MAS ^{1}H NMR and diffuse reflectance IR spectroscopy data, the distorted tetramethylammonium (TMA) cation and the Brønsted acid residue form the $(CH_3)_4N^+\cdots{}^-O-Si$ ion pair.[39] The content of the quaternary ammonium cation was found to be linearly correlated with the specific surface area (Fig. 4). The TMA cations are located on the surface of the new phase, although, as follows from NMR spectroscopy data, most of the quaternary base molecules are located in the bulk. The adsorbed quaternary base molecules occur at the gas/glass interface. The methyl groups of these molecules are free to rotate, since the nitrogen moiety is immersed into the bulk of the new phase, while CH_3 groups are exposed to the surface. The concentration of these molecules does not exceed 10% of the monolayer in the Al silicate glass fibre with a specific surface area of 16 m^2 g^{-1} (Ref. 39). The rotation of methyl

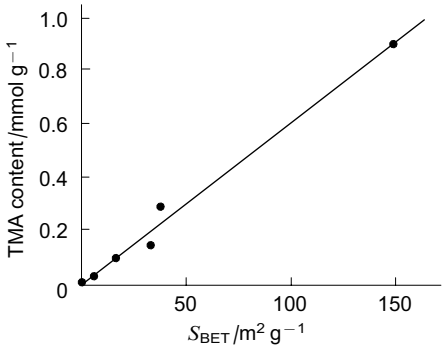


Figure 4. Content of TMA cations *vs.* specific surface area of glass fibres modified with a quaternary ammonium base.[39] S_{BET} is the Brunauer–Emmett–Teller specific surface area.

groups in TMA cations completely immersed into the gel-like phase is highly hampered because of the relatively high viscosity of the environment. As a result, the line in the NMR spectrum is anisotropically broadened; the higher the viscosity, the wider the line.[49] By varying the viscosity of aqueous glycerol solutions, it was possible to select the temperature and glycerol concentration such that the line width for the model solution coincided with the experimental one. As was to be expected, the gel-like phase viscosity of 7 kP proved to be markedly lower compared with that of initial glasses but ~20 times higher than that of pure glycerol and 4 orders of magnitude higher than the water viscosity.[39]

Thus, the hydrothermal treatment of GFs with an organic nitrogen base gives rise to a gel-like silicate phase on the surface with a thickness of several tens of nanometres. This phase is porous and has a lower viscosity. Depending on the GF nature and conditions of the hydrothermal treatment, its surface area varies from several square metres per gram to 149 $m^2 g^{-1}$ (Ref. 39). The gel-like phase contains a large number of $(CH_3)_4N^+ \cdots {}^-O-Si$ ion pairs on which, for example, dissociative adsorption of hydrogen sulfide molecules takes place. The $Si-O^-$ anionic residue is a strong base [the proton affinity (PA) is 1390 kJ mol^{-1}],[68] able to detach a proton from a hydrogen sulfide molecule (PA = 1477 kJ mol^{-1}). It is quite probable that the small difference $\Delta PA = 87$ kJ mol^{-1} would be easily counterbalanced by the electrostatic attraction between the $(CH_3)_4N^+$ cation and the HS^- anion. The quantitative data on H_2S absorption demonstrated that one such ion pair absorbs one hydrogen sulfide molecule. Some N-modified GF samples absorbed >2 mass % of hydrogen sulfide from a methane flow owing to strong interaction of H_2S with these ion pairs.

The desorption of H_2S in a dry methane flow was incomplete even when the temperature was raised to 80 – 100 °C, which accounted for the considerable imbalance between the absorbed and released hydrogen sulfide.[39] Evidently, this is caused by strong interaction of hydrogen sulfide with the ion pair. The situation crucially changes when desorption is carried out in a wet flow. In this case, the H_2S desorption rate sharply increases and the absorbed H_2S is entirely released at room temperature.[39] Presumably, a more polar water molecule displaces less polar hydrogen sulfide. Most likely, this process is affected by stronger binding of TMA to OH groups than to larger hydrogen sulfide anions.

4. Synthesis and properties of the Pd(Pt)/glass fibre catalysts

Methods for the synthesis of Pd(Pt)/GF catalysts and results of studying their properties by various physical methods have been described in detail;[22, 40, 41, 69, 70] therefore, we will mention only the milestones.

The key step of the synthesis of catalysts is ion exchange of transition metal cations with acidic protons of the bridging OH groups of glass.[40, 69] The unique feature of this reaction is that it takes place only in weakly alkaline medium and only with stable Pd^{2+} and Pt^{2+} ammonia complexes. Probably, the main cause for this is the ability of glass to absorb only polar molecules such as NH_3. Presumably, ligands (ammonia) diffuse first into the bulk of glass, and metal cations diffuse only thereafter. The attempts to introduce other metal cations from solutions of salts or complexes with other ligands into the bulk of glass fibres were unsuccessful.

In order to improve the mass transfer of platinum or palladium cations towards the fibre surface, a glass fabric impregnated with a solution of Pt^{2+} and Pd^{2+} ammonia complexes was wrung between special rollers. For avoiding fast evaporation, the sample was isolated from the environment and kept at low temperature for a long period of time. Thus, ion exchange was carried out under conditions that ensured the transfer of the greatest number of metal ions from the solution to the bulk of the glass. In order to avoid back transfer of platinum and palladium complexes from the glass fibre bulk to the surface, the metal cations were rapidly reduced. For this purpose, the sample was heated at a rate of approximately one Celsius degree per second up to 340 – 350 °C.[22, 40] The Pt^{2+} ions were reduced with NH_3 ligands with evolution of molecular nitrogen; therefore. no additional reduction of the catalyst was performed. The Pd^{2+} cations were reduced to the metal with a 1% solution of hydrazine at room temperature.[41]

Figure 5 illustrates two approaches to the synthesis of Pd/glass fibre catalysts. One approach is based on ion exchange between palladium or platinum cations and protons of the glass and the other one is based on impregnation with solutions of Pt^{2+} and Pd^{2+} ammonia complexes and deposition of anionic forms of a precursor. Studies of these catalysts by electron microscopy and ionic etching X-ray photoelectron spectroscopy (XPS) showed that in the former case, the highly dispersed 1 – 2 nm metal particles (designated as Pd_V) are confined in the bulk of glass fibres at a depth of up to 10 nm.[69, 70] When anionic palladium (platinum) species are used, no ion exchange obviously takes place and the metal is deposited almost entirely on the outer surface of the fibre as small 5 nm particles (designated as Pd_S). Indeed, the Pd_S concentration depth profile has a characteristic maximum at this size.[69, 70] Similar profiles were also observed in the case of platinum located in the bulk (Pt_V) and on the surface (Pt_S) of glass fibres.[40, 71] Unlike palladium, approximately one-fourth of the total amount of platinum in the catalyst exists as Pt^{2+} ions (Fig. 6 *a*).[40] It is important that neither high-temper-

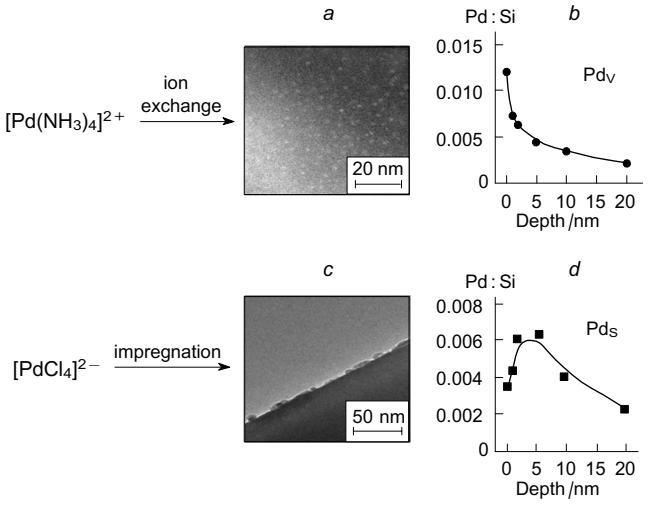


Figure 5. Two approaches to the synthesis of Pd/GF catalysts (*a*, *c*) and concentration depth profiles for Pd particles confined in the bulk (*b*) and deposited on the outer surface of the fibre (*d*).[40, 69 – 71]

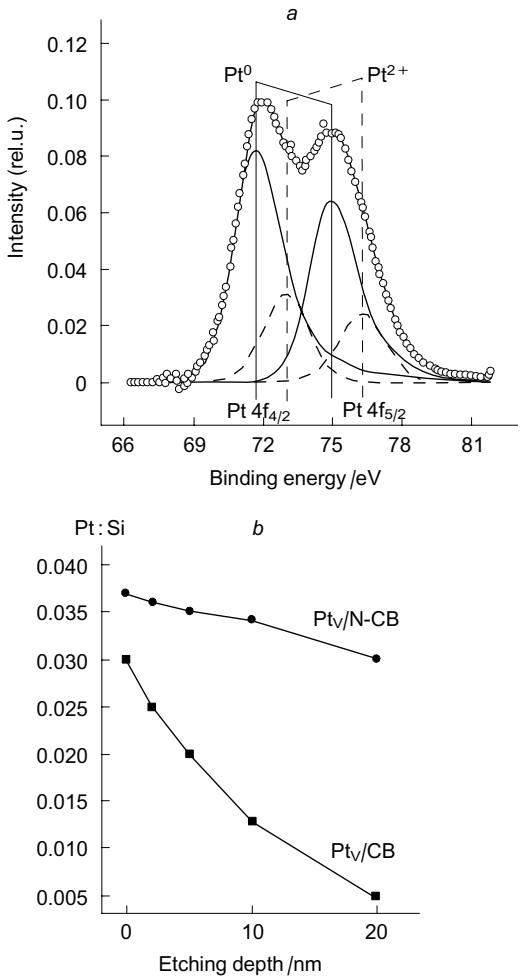


Figure 6. Pt 4f X-ray photoelectron spectrum of the Pt_V/GF catalyst normalized to the intensity of the Si 2p spectrum (*a*) and platinum concentration depth profiles for Pt_V/GF and Pt_V/N-GF (*b*).[40,71] (*a*) Dots are experimental data, continuous and dashed lines show deconvolution of the spectrum into two components for Pt^0 and Pt^{2+}, respectively.

ature treatment with hydrogen nor treatment with a hydrazine solution induced the reduction of these ions to metal. Presumably, platinum cations are incorporated in the platinum metal–oxide clusters and are not associated with partially reduced platinum oxide particles. Apart from the XPS data, the confinement of platinum clusters is confirmed by data of differential dissolution[72] of the Pt/Zr-GF catalyst.[73]

The other method was used to prepare catalysts in which the GF support was modified with an organic nitrogen base (N-GF). The synthesis was carried out under hydrothermal conditions for several days in an autoclave with a tetramethylammonium hydroxide solution and a palladium or platinum ammonia complex with the same concentration as used in the conventional glass fabric impregnation procedure.[40,60,69] The subsequent ion exchange and platinum or palladium reduction steps were carried out in the same way as in the synthesis of catalysts using non-modified glass fibres. Similarly, after the intramolecular Pt^{2+} reduction, approximately a quarter of platinum remained in the oxidized state.[40] Furthermore, the oxidized platinum was not reduced with hydrogen even at high temperature, while Pd^{2+} was completely reduced to metallic state with a 1% solution of hydrazine at room temperature.[41]

The Pt : Si (Fig. 6 *b*) and Pd : Si (not given) concentration depth profiles measured for both catalysts by XPS with ion etching proved to be different.[40,60] In the case of the N-modified catalyst, the metal concentration profile was much more gently sloping and was always located above the profile for the initial sample. This means that platinum is distributed over the film rather uniformly and is likely to be more dispersed than in the non-modified catalyst.

5. Selective hydrogenation of acetylene with Pd/glass fibre catalysts

The palladium-catalyzed selective hydrogenation of ethane–ethylene fractions is used to remove acetylene impurity (0.1%–1%) from ethylene.[74,75] Due to switching of industrial hydrotreating processes to the safe tail-end design (relatively low ratio $H_2 : C_2H_2 = 2–4$ and $C_2H_4 \gg C_2H_2$), the requirements to process selectivity became considerably more rigorous. Indeed, the selectivity to ethylene markedly increased upon the appearance of bimetallic catalysts (mainly Pd–Ag),[76–78] catalysts with single palladium atoms[79–83] and alloy systems with isolated palladium atoms.[78,84–87] There is no basic difference between the terms 'single' and 'isolated', but the latter just means that the palladium atom occurs in an intermetallic or alloy and is surrounded by atoms of another metal. However, the increase in the selectivity was accompanied by a clear downward trend of activity. This brought about the need to consider again the relationship between selectivity and activity in order to optimize the composition of Pd catalysts and to search for new catalytic systems.

In this Section, the activities (in terms of TOF) and selectivities of glass fibre catalysts and conventional mono- and bimetallic supported catalysts are compared over a broad range of dispersion degrees of palladium, including single Pd atoms. Particular attention is paid to the factors that determine the selectivity of acetylene hydrogenation. Using analysis of kinetic and isotope data,[41,70] the contributions of various reaction pathways to the reaction selectivity were quantitatively determined, the causes for higher selectivity of GF catalysts were identified and ways for increasing the selectivity were proposed.

Since Pd sites are confined in the bulk, it is assumed that reactants are transferred from the gas phase across the gas/glass interface and then diffuse towards the active sites. Therefore, it is necessary to compare the rates of the chemical (catalytic) reaction and diffusion of reactants in the glass fibre bulk. The confinement depth (h) for most active sites is 5–10 nm and the diffusion coefficient (D) at $T = 50$ °C slightly exceeds 6×10^{-11} cm^2 s^{-1} (Ref. 55). Then the time of diffusion

$$\tau = \frac{h^2}{D} \qquad (1)$$

is estimated as 10^{-2} s; this is two orders of magnitude smaller than the reaction turnover time (the reciprocal of TOF) measured at the same temperature.[70] Thus, the reactant diffusion in the bulk of glass is fast and cannot be the rate-limiting step for the catalytic reaction.

In order to identify the size effect in the palladium-catalyzed hydrogenation of acetylene, the TOF values were determined for nanoparticles with sizes in the 1–9 nm range, for subnanometre particles and for catalysts with

Table 1. TOF values for selective hydrogenation of acetylene in the presence of various palladium catalysts.

Catalyst	Pd content (mass %)	Size of Pd particles /nm	TOF /s^{-1}	Ref.
$Pd/\alpha\text{-}Al_2O_3$	0.05	4	0.38	88
$Pd/\alpha\text{-}Al_2O_3$	0.035	9	0.70	88
Pd/SiO_2	2.6	4.2	0.32	89
Pd/SiO_2	2.7	7.4	0.36	89
Pd/C	1	0.6	0.47	90
$Pd/\gamma\text{-}Al_2O_3$	1	0.8	0.54	90
Pd_S/CB	0.14	5	0.55	70
Pd – Ga	60 Pd : 40 Ga	Isolated Pd atoms	0.14	85
Pd_1/C_3N_4 (see [a])	0.5	Single Pd atoms	0.19	80
Pd_1/graphene [a]	0.25	Single Pd atoms	0.12	80
Pd_1/defective graphene [a]	0.11	Single Pd atoms	0.02	81
$Pd - Ag/SiO_2$	0.1 Pd : 4.76 Ag	Isolated Pd atoms	0.20	78
Pd_V/CB	0.02	1.5	0.13	70
Pd_V/N-CB	0.02	1.5	0.48	54
$Pd - Ag/Al_2O_3$	0.05 Pd : 3.1 Ag	–	0.75	54

[a] Pd_1 is the designation for a single palladium atom.

single atoms (Table 1). In our opinion, it is most important to study the structure sensitivity of this reaction on going to subnanometre size and especially to single atoms. The TOF values for acetylene hydrogenation on single Pd atoms, although determined in several studies, have never been compared with analogous data for larger metal particles. The experimental data on selective hydrogenation of acetylene were obtained for a rather narrow temperature range (25 – 75 °C) and for compositions of the feed gas close to tail-end conditions (see above), that is, for large excess of ethylene and a moderate $H_2 : C_2H_2$ ratio. The kinetics of palladium-catalyzed selective hydrogenation was thoroughly studied exactly for this concentration and temperature ranges and adequately reflected the existing views on the reaction mechanism. In particular, the reaction was first order with respect to hydrogen and zero order with respect to acetylene, and the activation energy was close to 40 kJ mol^{-1} (Refs 70, 80, 91 – 94). The zero order with respect to C_2H_2 is due to high heat of acetylene adsorption, while the first order with respect to H_2 is due to the dissociative adsorption of molecular hydrogen, that is, the reaction proceeds at low hydrogen coverages and high acetylene coverages. This allowed correct comparison of TOF values for the reactions under identical conditions, which were chosen to be $T = 55$ °C and hydrogen partial pressure of 0.07 bar. In most cases, the concentration of surface palladium atoms, which is needed to calculate TOF, is found by $O_2 - H_2$ titration and/or from the data on the degree of dispersion of Pd nanoparticles.[70, 90] For the bimetallic $Pd - Ag/Al_2O_3$ catalyst, it was determined from the low-temperature IR spectra of adsorbed CO.

The data presented in Table 1 indicate that the turnover frequencies for acetylene hydrogenation catalyzed by various palladium particles with an average size from 1 to 9 nm fall in a relatively narrow range of 0.3 – 0.7 s^{-1}. In other words, TOF depends little on the degree of dispersion of Pd particles and the nature of the support (aluminium and silicon oxides, carbon and silicate glass fibres). In other words, this reaction is structure-insensitive. Hence, the rate-limiting step is the addition of adsorbed hydrogen to the alkyl complex;[93] in this case, adsorbed acetylene.[85, 92, 94] This is in good agreement with published data on the hydrogenation of unsaturated hydrocarbons in the presence of supported metal (mainly Pd and Pt) catalysts (see, for example, Ref. 84). Both glass fibre catalysts, Pd_S/GF and Pd_V/N-GF, also fall in the above range of turnover frequencies, although TOF is somewhat lower for non-modified Pd_V/GF. It is noteworthy that palladium deposition on the GF surface does not give any benefits in the reaction rate. Nevertheless, Pd_S/GF can compete with supported palladium catalysts, because it also has the technological advantage of possibility to fabricate flexible structured catalyst layers of virtually any shape.[3, 4] However, the problems associated with adhesion between the metal (or oxide) to the glass fibre are inevitable, because metal crystallites can hardly interact with glass. Glass fibre catalysts of this type may lose activity either due to agglomeration of particles of the active component or due to leaching.

The TOF values for the reactions with catalysts comprising single or isolated palladium atoms proved to be markedly lower than those for Pd nanoparticles, in particular, 0.12, 0.19 and 0.14 s^{-1} for Pd_1/graphene, Pd_1/C_3N_4 (Ref. 80) and Pd – Ga intermetallic compounds, respectively.[85] In the case of single palladium atoms deposited on defective graphene, the TOF decreased to 0.02 s^{-1} (Ref. 81), which is more than an order of magnitude lower than those for most Pd supported catalysts. Larger scatter of TOF values in the case of single atoms is apparently due to the fact that the Pd_1 electronic state and local environment depend to a larger extent on the nature of the support and its interaction with the palladium atom. In these studies, reaction conditions (hydrogen pressure and temperature) were close to those chosen above. Therefore, lower TOF values for single palladium atoms compared to those for Pd supported catalysts (see Table 1) are, most likely, attributable to a change in the reaction mechanism.

In the case of acetylene hydrogenation catalyzed by supported bimetallic alloys, it was difficult to determine TOF, because either kinetic data or data on the number of surface palladium atoms were missing. These data are presented in most detail by Pei *et al.*,[78] who comprehensively studied the $Pd - Ag/SiO_2$ catalysts with isolated palladium atoms. The concentration of surface palladium atoms determined from IR spectroscopy data for adsorbed CO amounted to 2.4 μmol g^{-1}. For this purpose, the intensity of the CO absorption band (0.0007) was measured at full width at half maximum of 70 cm^{-1}, and the integrated absorption coefficient for CO linearly adsorbed on palladium (20 cm μmol^{-1}) was taken from Ref. 95. The reaction rate equal to 0.5 μmol s^{-1} g^{-1} was calculated at 55 °C from the temperature dependence of conversion in the differential reactor approximation. This gave TOF = 0.2 s^{-1}, which is virtually equal to the turnover frequency for the Pd_1/C_3N_4 catalyst.

Thus, in the case of single or isolated palladium atoms, there is a clear trend towards decreasing specific rate of the reaction or the turnover frequency. This brings about an important question of whether the hydrogenation reaction is still structure-insensitive in the subnanometre region and especially when hydrogenation proceeds on single atoms? The TOF values for the Pd/C catalyst [90] with subnanometre particles consisting of several atoms well fit into the above-

mentioned range of invariable TOF values for Pd nanoparticles. However, for ethylene hydrogenation catalyzed by Pt_n clusters (n is the cluster dimensionality) supported on magnesium oxide, it was shown that in the range of $n = 8-15$, the reaction becomes structure-sensitive, with a clear-cut TOF maximum being observed for $n = 13$; further decrease in the cluster dimensionality entailed a decrease in the reaction rate.[96] Molecular hydrogen ($H_2 + D_2$) was dissociatively adsorbed on platinum clusters, since their activity was well correlated with the measured intensity of the HD ion mass.

The preliminary high-temperature treatment of catalysts (> 130 °C) resulted in the formation of carbon structures (ethylidyne, $\equiv$CH), and hydrogenation became again structure-insensitive. Indeed, the TOF coincided with that for the reaction on the Pt(111) surface. Hence, the formation of carbon deposits is a necessary condition for structure insensitivity of the hydrogenation reaction, at least, in the area of particle size < 1 nm. Apparently, carbon dilutes Pd atoms and transfers electron density to them;[86] as a result, palladium atoms become similar to those in bimetallic alloy systems. It cannot be ruled out that adsorbed hydrogen atoms migrate over the surface of the carbonized support towards adsorbed ethylene, and this accounts for the structure insensitivity of the reaction.

The decrease in the turnover frequency of a reaction on catalysts with single atoms may be caused by retardation or even suppression of dissociation of molecular hydrogen, since a less reactive atom of the support such as carbon or oxygen serves as the second atom. Recently, interesting data have been obtained on the hydrogenation of propylene on single platinum atoms strongly attached to a Keggin-type P–Mo heteropolyacid, which was in turn supported on active carbon.[97] Unlike single Pd atoms on various supports, in this case, platinum atoms are structurally and electronically uniform and cannot agglomerate during the reaction, as one Pt atom is attached to one heteropolyacid molecule. Evidently, diffusion of active intermediates, in particular hydrogen, is unlikely in this case. It was found that platinum atoms whose binding energy to the support is similar to the binding energy in platinum metal are the most stable and active. Meanwhile, dissociation of H_2 cannot proceed on single platinum atoms even with participation of the neighbouring oxygen atoms.[97]

It was assumed that propylene and molecular hydrogen are adsorbed on a platinum atom, and hydrogenation takes place, first to the isopropyl intermediate and then to propane, the last step being the rate-limiting one. This hydrogenation mechanism involving a single Pt atom differs fundamentally from the known reaction mechanism on the surface of a metal nanoparticle in which dissociative adsorption of hydrogen is the key step. Similar homolytic H–H bond cleavage on the central atom of the complex is common in homogeneous catalysis.[98] Thus, the decrease in TOF on going to single atoms is due, most likely, to the change in the mechanism of hydrogenation of unsaturated hydrocarbons. Note that in a previous study of propyne hydrogenation on a Pd_V/GF catalyst by parahydrogen-induced polarization, it was found that a considerable portion of hydrogen adds to the triple bond in a pairwise manner, *i.e.*, the two H atoms come from the same H_2 molecule.[99] Of course, this does not mean a change in the reaction mechanism, as in the previous case, but means that hydrogen atoms cannot migrate over long distances, since glass can confine highly dispersed metal clusters in a narrow space. Therefore, the probability that two hydrogen atoms from the same H_2 molecule add to acetylene substantially increases in comparison with supported Pd catalysts.

Meanwhile, the reaction selectivity, or an increment in ethylene with respect to converted acetylene, significantly increases with increasing degree of dispersion of Pd particles. The fact is that the acetylene and ethylene adsorption energies considerably decrease on highly dispersed palladium particles.[78,80–83] Therefore, even for high acetylene conversions, the highest selectivity is observed for catalysts based on single Pd atoms; under these conditions, weakly bound acetylene and ethylene are desorbed to the gas phase more rapidly than they could be hydrogenated to ethane. Indeed, the Pd_1/graphene and Pd_1/C_3N_4 catalysts showed selectivities of 80% and 90%, respectively, near complete conversion of acetylene.[80] Nevertheless, the selectivity can decrease because of hydrogenation of excess ethylene present in the gas phase. This is related to thermodynamic factors, particularly, a much higher heat of acetylene adsorption on palladium compared with ethylene.[75,92] Therefore, at high acetylene conversions, the selectivity sharply decreases, because acetylene is gradually released from the palladium surface, and gas-phase ethylene starts to be hydrogenated to ethane. Indeed, the selectivity of the Pd_S/GF catalyst decreases almost to zero as approaching complete conversion (Fig. 7), which is typical of monometallic catalysts.[75,100–103] The sharp decrease in the selectivity as a result of hydrogenation of gas-phase ethylene was previously confirmed by isotope labelling.[104] However, in the case of the Pd_V/GF catalyst, in which palladium is confined in the glass bulk, the reaction selectivity slightly changes with conversion, but remains high up to complete conversion of acetylene (Fig. 8).

Indeed, the selectivities of the glass fibre-based and bimetallic catalysts remain high even when acetylene conversion is > 99% and the ethylene concentration is 4–5 orders of magnitude higher than the concentration of acetylene.

The points in Fig. 8 corresponding to 100% conversion of acetylene mean that their residual concentration is ⩽ 3 ppm (sensitivity of chromatographic analysis). The situation looks as if gas-phase ethylene was not hydrogenated at all, but was only formed from acetylene. Therefore, it is important to determine the contributions of the two pathways towards ethane to the reaction selectivity, especially at high conversions:

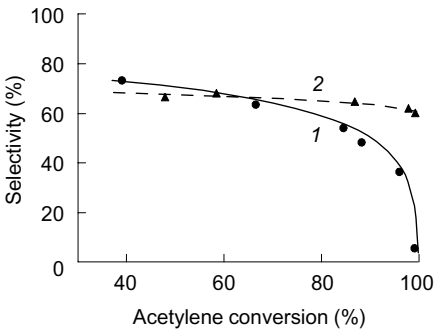


Figure 7. Selectivity *vs.* conversion for acetylene hydrogenation reaction catalyzed by 0.14% Pd_S/GF (*1*) and 0.02% Pd_V/GF (*2*) at 65 and 85°C, respectively.[70] Initial mixture/vol.%: 2.0 C_2H_2 + 2.0 C_2H_4 + 7.0 H_2 + He; $P = 1$ bar.

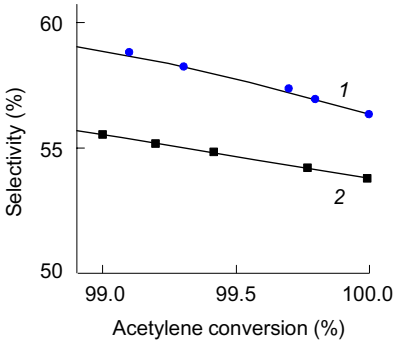


Figure 8. Selectivity *vs.* conversion for acetylene hydrogenation reaction catalyzed by Pd_V/GF (*1*) and Pd – Ag/Al_2O_3 (*2*).[54] Initial mixture /vol.%: 0.53 C_2H_2 + 59.0 C_2H_4 + 0.78 H_2 + Ar, P = 20 bar, T = 77 °C.

— successive hydrogenations of acetylene and ethylene;
— hydrogenation of gas-phase ethylene.

For this purpose, kinetic measurements were carried out by the SSITKA method [37, 105] using two catalysts: Pd_V/GF containing 0.02% palladium in the bulk and Pd_S/GF containing 0.14% palladium on the outer surface of glass fibres. Under steady-state conditions at an invariable acetylene conversion of 97% – 99%, $^{12}C_2H_2$ was replaced in a stepwise manner by $^{13}C_2H_2$, and the transfer of ^{13}C isotope label from acetylene to the reaction products (ethylene and ethane) was measured experimentally. As a result, the percentages of ethane formed along both pathways were quantitatively determined.[70]

In the case of Pd_S/GF, the ^{13}C-labelled fraction of ethane (α) was 55%, that is, approximately half of ethane was formed by successive acetylene and ethylene hydrogenation reactions and the rest was formed upon hydrogenation of the gas-phase ethylene. In the case of the Pd_V/GF catalyst, $\alpha = 96 \pm 3\%$, *i.e.*, ethane is most entirely formed from acetylene. In other words, gas-phase ethylene is almost not hydrogenated.[70] This is due to poor solubility of ethylene in glass, rather than to the low binding energy of C_2H_4 to palladium. As a result, the selectivity of the Pd_V/GF catalyst is determined by only the proper catalytic reaction. However, the selectivity is moderate ($\sim$57%) compaired with that for Pd_1/graphene ($\geqslant$ 90%), which is caused by a noticeable contribution of the pathway of acetylene hydrogenation to ethane on relatively large (1 – 2 nm) Pd particles. In other words, the lifetime of adsorbed ethylene is sufficiently long, so that a major part of ethylene has time to be converted to ethane before being desorbed to the gas phase.

For quantitative characterization of this reaction pathway, the intrinsic selectivity ${}^*S_{C_2H_4}$ was introduced [104] as the ratio of the amount of ethylene formed from acetylene to the amount of converted acetylene

$$ {}^*S_{C_2H_4} = \frac{{}^*C_{C_2H_4}}{{}^*C_{C_2H_4} + {}^*C_{C_2H_6} + {}^*C_{C_4}} \qquad (2) $$

where ${}^*C_i$ is the concentration of carbon-labelled hydrocarbons. In essence, this is the contribution of the proper catalytic reaction to the overall selectivity without taking account of the pathway of hydrogenation of gas-phase ethylene.

In the case of the Pd_S/GF catalyst, the intrinsic selectivity for 97% conversion of acetylene was 54%, *i.e.*, approximately half of ethane was formed from acetylene, while the other ethane was formed from gas-phase ethylene.[70] As the acetylene conversion approached 100%, hydrogenation of gas-phase ethylene became the predominant pathway and the overall selectivity decreased almost to zero. In the case of Pd_V/GF, the intrinsic selectivity was $\sim$59%, which is close to that for Pd_S/GF, although measured at a higher acetylene conversion (99%).[41, 70] It should be emphasized that the intrinsic selectivity is close to the overall one, since gas-phase ethylene does not participate in the reaction, which well accounts for the smooth dependence of the selectivity on conversion (see Fig. 7). As was to be expected, the intrinsic selectivities of both catalysts are similar and do not depend on the size of Pd particles, which confirms once again the structure insensitivity of the hydrogenation reaction.

Transition to subnanometre Pd particles and then to single atoms increases the intrinsic selectivity by decreasing the binding energy of intermediate ethylene species. It was noted above that the key shortcoming of single-atom catalysts is low reaction rate. It does not matter whether the reaction rate is expressed in terms of TOF, or expressed per unit volume or weight of the catalyst, since the atomic dispersion is mainly associated with a low metal content in the catalyst. In addition, the binding energy between Pd_1 and the support may be not high enough to avoid agglomeration of atoms into larger clusters during the reaction,[106] which would lead to selectivity loss.

For bimetallic catalysts, the selectivity – activity relationship is more complicated. The Pd – Ga intermetallic compounds with single palladium atoms demonstrate the same trends as Pd_1 catalysts, that is, high selectivity and a low TOF equal to 0.14 s^{-1} (see Table 1). In the Pd – Ag alloy, single palladium atoms have higher electron density due to the donor properties of silver. In view of this, a high selectivity can be expected, because the contributions of both undesirable pathways are minimized. However, the bimetallic catalyst showed a moderate selectivity (54%) for complete acetylene conversion (see Fig. 8), but a high activity. Probably, this is attributable to segregation of the surface palladium atoms to give larger Pd clusters, which is enhanced on contact with the reaction medium, especially with acetylene.[107, 108] The similarity of the selectivity *vs.* conversion dependences for the Pd – Ag/Al_2O_3 and Pd_V/GF catalysts suggests that the decrease in the selectivity is caused by a pronounced contribution of acetylene hydrogenation giving ethane, which is virtually absent in the case of single atoms. Certainly, a contribution of hydrogenation of the gas-phase ethylene on palladium clusters cannot be ruled out either. Therefore, glass fibre catalysts Pd_V/GF and especially Pd_V/N-GF are more promising due to the specific ability of glass not to dissolve non-polar molecules and confine metal clusters. This completely excludes the gas-phase ethylene hydrogenation pathway, and no agglomeration of metal particles confined in the glass bulk takes place. For improving the selectivity, one should merely increase the degree of dispersion of Pd particles, which would reduce the contribution of acetylene hydrogenation to ethane.

In conclusion, let us mention the stability of the palladium catalysts for selective hydrogenation of acetylene. It is known that deactivation of supported Pd catalysts is based on acetylene oligomerization to give high-boiling products,

so-called green oil.[109] Since these reactions are initiated by strong adsorption of acetylene, the selectivity is well correlated with stability: the higher the intrinsic selectivity, the more stable the catalyst. The catalyst deactivation is slow; therefore, the appearance of C_4 dimers is indicative of formation of large amounts of oligomers. The long-term testing of the Pd_V/GF catalyst demonstrated that the catalyst activity remained invariable for at least 100 h and only trace amounts of butenes and butadiene were formed.

6. Complete oxidation of hydrocarbons on the Pt/glass fibre catalysts

Complete oxidation of hydrocarbons taking place on supported metal and oxide catalysts is involved in the catalytic treatment of gas emissions containing hazardous VOCs.[110, 111] Due to higher activity, this process is mainly carried out with supported Pt(Pd)/Al_2O_3 catalysts, both granulated and monolith ones with platinum or palladium content of 0.2 mass % – 0.6 mass %. The key drawbacks of these catalysts are low stability to the action of poisons (P, S and other impurities) and high cost due to the presence of noble metals.[110] As a rule, a decrease in the platinum metal content in the catalyst increases the degree of dispersion. In small particles, coordinatively unsaturated atoms prevail, which easily form strongly bound but relatively unreactive oxygen. This decreases not only the platinum content, but also the catalyst activity in the deep oxidation of hydrocarbons.[112] Hence, it is necessary to solve simultaneously two mutually exclusive problems, namely, to decrease the platinum content in the catalyst and to increase the activity, which seems to be quite a challenge. In addition, it is necessary to increase the stability of the catalyst to catalyst poisons contained in gas flows.

The kinetic and isotope studies of the deep oxidation of hydrocarbons catalyzed by Pt/GFs are described in detail in our publications.[22, 40, 69, 71] In this Section, the attention is focused on the correct comparison of activities (TOFs) of glass fibre catalysts and supported platinum catalysts, size effects and structure sensitivity of the Pt-catalyzed deep oxidation of propane. Also, the effect of the platinum oxidation state on the catalyst activity is discussed and ways for improving the catalyst are proposed.

The rates of complete oxidation of n-butane on Pt/GF catalysts depending on the location of platinum in the glass fibre are summarized in Table 2.[22]

For the calculation of TOF, the concentration of the surface platinum atoms was determined from data on the degree of dispersion of particles, while in the case of Pt_V/GF catalysts, the total platinum content was used. Although the platinum concentration in the GF catalysts was 2 – 3 orders of magnitude lower than in the reference sample, the reaction rate per unit weight of the catalyst proved to be 2 – 3 times higher. The TOF values for the Pt_V/GF catalyst were more than an order of magnitude higher than those for the reference sample, which is indicative of a clear-cut structure sensitivity of the reaction. Meanwhile, the turnover frequency of the Pt_S/GF catalyst (platinum particles are deposited on the GF outer surface) was close to the TOF for the reference catalyst.[22] Like in the case of palladium, this proves once again that the use of glass fibres as the support for metal particles does not provide any gain in the activity in comparison with traditional oxide supports. However, this brings about a problem of low strength of the metal – glass contact and, as a consequence, quite probable deactivation of Pt_S/GF catalysts because of either agglomeration of platinum particles or carrying away of the particles with the gas flow. Meanwhile, the Pt_V/GF catalysts showed a high thermal stability and did not lose activity after high-temperature treatment.[22, 23]

Table 2. Characteristics of the activity of platinum catalysts during complete oxidation of n-butane (feed gas 0.2% C_4H_{10} in air, $X_{C_4H_{10}} = 60\%$, $T = 400$ °C).[22]

Catalyst	Pt content (mass %)	Average size of Pd particles /nm	Reaction rate /μmol g^{-1} s^1	TOF /s^{-1}
Pt/Al_2O_3 [a]	0.56	8	1.3	0.8
Pt_S/CB	0.22	6	2.9	0.8
Pt_V/CB	0.01	1 – 2	4.2	8.4
Pt_V/CB	0.003	⩽ 1	2.2	14.7

[a] Commercial catalyst AP-56.

Considering the confinement of Pt sites, mass transfer of reactants from the gas phase across the gas/glass fibre interface and their subsequent diffusion towards active sites are assumed. Therefore, it is necessary to compare the rates of the chemical (catalytic) reaction and reactant diffusion in the bulk of glass fibre. Most of active sites are located at a depth of 5 – 10 cm; since the diffusion coefficient at 400 °C is $\sim 10^{-8}$ nm^2 s^{-1} (Ref. 56), the time of diffusion can be estimated to be of the order of magnitude of 10^{-4} s. This is 1000 times shorter than the characteristic time of n-butane oxidation, the reciprocal of TOF equal to 0.1 s; that is, diffusion in glass proceeds much faster than the catalytic reaction.[22]

Glass fibre catalysts are much more active than the industrial catalyst AP-56 (Fig. 9).[69] Despite 30 times lower content of platinum, the half-conversion temperatures of toluene on the Pt_V/GF and Pt_V/N-GF catalysts are lower than those on the industrial catalyst by 40 and 70 °C, respectively. A remarkable fact is that the quite stable organic compound is oxidized to CO_2 and H_2O at temperatures considerably below 100 °C. Similar results were observed for the oxidation of toluene on the active catalyst 0.2% Pt/SBA-15,[113] although the reaction started only at 100 °C. It was found that subnanosized low-coordinate Pt atoms located in the mesopores of the support are able to cleave the C – C bond in adsorbed toluene to give phenyl and methyl intermediates, which are then easily oxidized by

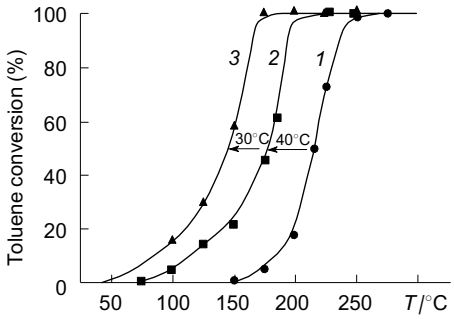


Figure 9. Temperature dependences of the activity of platinum catalysts in complete oxidation of toluene.[69] (*1*) AP-56, (*2*) 0.02% Pt_V/GF, (*3*) 0.02% Pt_V/N-GF. Feed gas /vol.%: 0.1 C_7H_8 + 20 O_2 + N_2; space velocity: 8000 h^{-1}.

oxygen to complete oxidation products. Assuming the first-order kinetics with respect to toluene, the TOF values for Pt_V/GF and Pt_V/N-GF catalysts at $T = 110$ °C can be found from the data presented in Fig. 9 (curves *2* and *3*) to be 0.08 and 0.17 s^{-1}; this is close to 0.1 s^{-1}, which is the TOF value for 0.2% Pt/SBA-15. This may be indicative of similar mechanisms of toluene oxidation on both catalysts.

The next example concerns the complete oxidation of methane catalyzed by Pt_V/GF at the stoichiometric reactant ratio: $CH_4 : O_2 = 1 : 2$. As can be seen in Fig. 10, the reaction starts at 450 °C and then stoichiometric oxidation of methane takes place until the reactants are completely exhausted.[114] Indeed, the reaction is almost terminated as the oxygen concentration decreases to ~0.001 vol.%; no other products except for CO_2 and H_2O are formed. This result can be practically used to recover nitrogen from air without the use of cryogenic processes. Glass fibre catalysts also showed high activity towards the removal of other VOCs (*e.g.*, ethylbenzene).[71]

It is of considerable interest to compare the activities of Pt_V/GF and Pt/Al_2O_3 and also samples containing platinum modified with electronegative dopants as catalysts for deep oxidation of hydrocarbons. These materials are prototypes of many industrial catalysts for the removal of hazardous VOCs from exhaust gases. It is very important to compare the turnover frequencies for the oxidation of propane on different catalysts. Table 3 presents TOFs for the complete oxidation of propane on Pt catalysts[40, 115–126] supported on various materials: alumina,[115–121] titania,[119] ceria,[119] aluminium fluoride,[122] silicon dioxide,[123] strontium titanate,[124] zeolite,[125] boron nitride[126] and glass fibre.[40] Some Al_2O_3-based catalysts were promoted by tungsten,[115, 118, 127] iron[121] and vanadium[123, 128] oxides and SO_4^{2-} anions.[116] The average size of Pt particles varied over a broad range from 1 to 18 nm and the metal content varied from 0.01% to 15%. It should be noted that the specific reaction rates (or TOF) were determined in most studies (in Table 3, they are designated by the superscript 'a'); in other of the cited studies, the reaction rate was estimated at low propane conversions directly from the conversion *vs.* temperature plots.

Since the reaction conditions were considerably different ($T = 200–300$ °C, $C_{C_3H_8} = 0.08\%–2\%$, $C_{O_2} = 2\%–20\%$), the turnover frequencies were compared under the following identical conditions: reaction temperature of 250 °C and propane and oxygen concentrations of 0.2% and 15%,

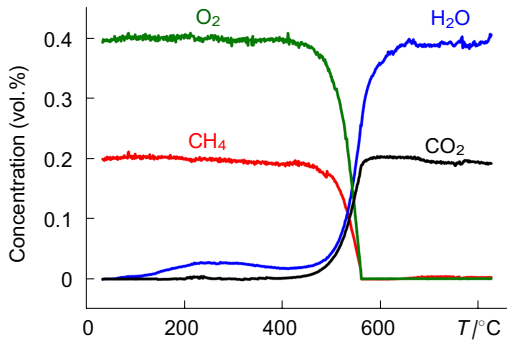


Figure 10. Temperature programmed complete oxidation of methane in the presence of the Pt_V/GF catalyst.[114] Feed gas /vol.%: 0.20 CH_4 + 0.40 O_2 + N_2 (for the balance); space velocity: 12 000 h^{-1}, heating rate: 10 °C min^{-1}.

Table 3. TOF for the complete oxidation of propane in the presence of Pt catalysts.

Catalyst	Pd content /(mass %)	Size of Pd particles /nm	TOF /s^{-1}	Ref.
		Group 1		
Pt/Al_2O_3	5	3	0.02	115
Pt/Al_2O_3	0.88	3.2	0.01	116
Pt/Al_2O_3	0.8	5.8	0.015	117 [a]
Pt/Al_2O_3	1.0	1.5	0.02	118
Pt/Al_2O_3	0.51	1.9	0.01	119 [a]
Pt/Al_2O_3	2.0	18	0.13	120 [a]
Pt/Al_2O_3	1.0	14	0.08	122
Pt/Al_2O_3	1.0	11	0.07	123 [a]
Pt_S/CB	0.12	5	0.007	40 [a]
		Group 2		
PtW/Al_2O_3	5 (W : Pt = 4)	6.6	0.27	115
$Pt/Al_2O_3SO_4$	0.88 (S : Pt = 10.9)	3.2	0.09	116
$Pt/WO_x/Al_2O_3$	1.0 (W : Al = 8.8)	1.5	0.11	118
Pt/CeO_2	0.49	2.3	0.04	119 [a]
Pt/TiO_2	0.48	3.8	0.08	119 [a]
$PtFe/Al_2O_3$	1.0 (Fe : Pt = 5)	17	0.12	121
Pt/AlF_3	0.17	1.6	0.04	122 [a]
Pt/SiO_2	1.95	3.0	0.01	123 [a]
$PtVO_x/SiO_2$	1.92	2.8	0.11	123 [a]
		Group 3		
$Pt/SrTiO_3$	15.2	4.5	0.61	124 [a]
Pt/USY	1.0	4.6	0.59	125 [a]
Pt/h-BN	0.5	2.1	0.33	126 [a]
Pt_V/CB	0.01	1–2	0.24	40 [a]
Pt_V/N-CB	0.01	1–2	0.30	40 [a]

[a] Publications in which the TOF values are reported; in other publications the reaction rate was estimated from the plots for the temperature dependence of conversion.

respectively. This comparison became possible owing to detailed investigation of the kinetics of this reaction on platinum catalysts. In particular, the extremal dependences of the reaction rates on the $O_2 : C_3H_8$ ratio[112, 120, 129, 130] and the changes in the order of reaction and activation energy with the variation of oxygen concentration were elucidated and interpreted. When the reactant ratio is high (> 8) and the platinum surface is saturated with chemisorbed oxygen, the order of reaction with respect to oxygen is zero while that with respect to propane is unity. Under these conditions, the rate-limiting step is dissociative adsorption of propane, which is followed by C—H bond activation and cleavage.[112, 118–120]

As the $O_2 : C_3H_8$ ratio decreases, the oxygen coverage decreases, the platinum surface is liberated for the adsorption of propane and the reaction rate increases. The order of the reaction with respect to oxygen becomes negative;[119, 120, 130] in the case of Pt/zeolite (Ref. 125) and Pt/TiO_2 (Ref. 119), it is close to −1, which is attributable to high concentration of adsorbed propane. The extremal dependences of the reaction rate on the oxygen concentration corresponding to different kinetic regimes are depicted in Fig. 11.[120, 130]

The order of the reaction with respect to oxygen varies from zero (high reactant ratio, $O_2 : C_3H_8 > 8$) to −1.5 (medium ratio, $1 < O_2 : C_3H_8 < 8$), whereas the order of

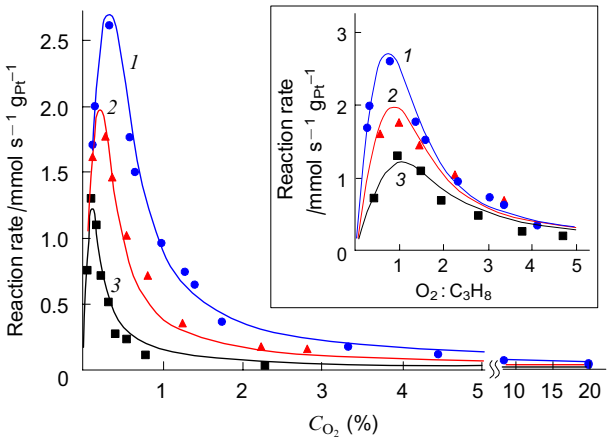


Figure 11. Reaction rate at 198 °C in the presence of Pt_V/GF *vs.* oxygen content for propane concentrations: 0.42 (*1*), 0.24 (*2*), 0.10 vol.% (*3*).[130] The inset shows the same dependences plotted in different coordinates. Dots are experimental data and lines are calculations according to the model.

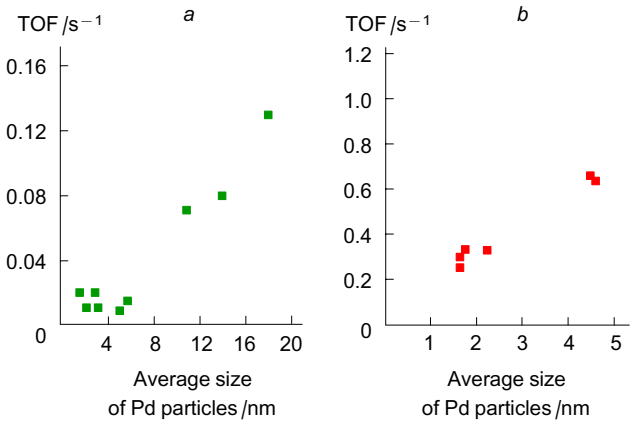


Figure 12. Size effect for total oxidation of propane with platinum catalysts of group 1 (*a*) and group 3 (*b*).[40,115–126]

the reaction with respect to propane remains to be unity until the $O_2 : C_3H_8 \approx 1$ ratio corresponding to the highest reaction rate is reached. Therefore, for the chosen conditions, the order of the reaction with respect to propane was taken to be 1 and that with respect to oxygen was taken to be 0 or −1.5, depending on the $O_2 : C_3H_8$ ratio. If the kinetics was known, TOF was calculated according to the kinetic equation. The observed activation energy in the presence of excess oxygen was 71 kJ mol^{-1}, while for medium $O_2 : C_3H_8$ ratios, the activation energy increased to 79 kJ mol^{-1}. Similar activation energies were found in another study,[119] with the value for zeolite catalysts being higher and amounting to 117 kJ mol^{-1}. Therefore, the authors, who did not determine the activation energy, adjusted the TOF values to a temperature of 250 °C using the activation energy of 71 (more rarely 79) kJ mol^{-1}. The fraction of surface platinum atoms was found, in most cases, from the data on chemisorption of H_2 or CO and from the degree of dispersion of Pt particles determined by electron microscopy (the results of both methods coincided).

From the results given in Table 3, it follows that the turnover frequencies differ by more than two orders of magnitude. In terms of TOFs, the catalysts can be conventionally divided into three large groups:

— group 1: catalysts prepared using alumina; reactions proceed slowly (TOF = 10^{-3}–10^{-2} s^{-1});

— group 2: catalysts modified by sulfates and oxides of tungsten (WO_x), vanadium (VO_x) and iron (FeO); the turnover frequencies are medium (TOF is of the order of magnitude of 10^{-2}–10^{-1} s^{-1});

— group 3: catalysts with platinum supported on zeolites, strontium titanate, boron nitride and silicate glass fibres able to efficiently polarize and activate the C–H bond in the propane molecule; the reactions are fast (TOF = 10^{-1}–10^{0} s^{-1}).

The turnover frequency of the Pt/Al_2O_3 catalyst linearly increases with increasing platinum particle size (Fig. 12 *a*), which is attributable to increasing fraction of the active metal phase able to adsorb reactive oxygen.[112,117,131,132] This result is indicative of clear-cut structure sensitivity of the reaction. It is known that small Pt clusters contain large amounts of low-coordinate platinum atoms, which form strongly bound and, hence, relatively unreactive oxygen species.[131] Meanwhile, the dissociative adsorption and subsequent oxidation of propane require several platinum atoms capable of activating hydrocarbon and oxygen molecules rather than one atom. Therefore, in small clusters (< 2 nm), the number of adsorption sites for propane and oxygen is relatively small and the reaction rate is low. According to the molecular views on structure sensitivity,[93] activation of these molecules requires so-called step-edge sites, the density of which decreases with decreasing platinum particle size. Therefore, the adsorption of propane and molecular oxygen and, as a consequence, the reaction rate, also decrease. Relatively large platinum particles, in which the density of these sites is higher, will be the most active. Unfortunately, in this case, the platinum content in the catalyst should also increase.

It is noteworthy that the activity of the Pt_S/GF catalyst, in which the platinum particles are deposited on the surface of glass fibre, is comparable with the activity of Pt/Al_2O_3 and corresponds to the size dependence of TOF for group 1 catalysts (Fig. 12 *a*). In small particles, the density of defective (low-coordinate) platinum states is high; therefore, they are highly sensitive to the conditions and preparation methods and also to various impurities that can be adsorbed on these sites and block them. Therefore, the ratio of defective and regular sites varies over a wide range, which, apparently, can account for the large scatter of activity values for ~1–2 nm particles.

To stabilize the metallic state of platinum under oxidative conditions and increase the reaction rate, the Pt/Al_2O_3 catalyst is doped with various electrophilic agents [115,118,121] or promoted with sulfates.[115,133] In both cases, this 'acid' treatment of platinum considerably increases the activity of modified catalysts (see Table 3, group 2). The introduction of electronegative tungsten oxide into Pt/SiO_2–Al_2O_3,[110] Pt/Al_2O_3 (Ref. 116) or Pt/BN (Ref. 134) resulted in a sharp increase in TOF, irrespective of the nature of the support. The promoting role of tungsten was attributed to its electrostatic interaction with platinum and formation of $Pt^{\delta+}$–WO_x pair sites at the metal/support interface; these sites can polarize and weaken the C–H bond in the propane molecule.[112,118–120,134,135] The addition of iron oxide slightly promoted the platinum activity, but increased the stability of particles against sintering.[121] Similarly to the

action of tungsten, sulfation of the catalyst also resulted in the generation of charged $Pt^{\delta+}$ atoms as a result of electron density withdrawal from the periphery of Pt particles by adjacent electronegative SO_4^{2-} anions located on alumina[116, 129] or mixed CeO_2-ZrO_2 oxide.[135] As a result, platinum atoms were positively charged and the $Pt^{\delta+}-WO_x(SO_4^{2-})$ pairs formed at the periphery of the metal particle. Propane molecules were dissociatively adsorbed on these sites; as a result, the C–H bond was weakened due to polarization, which resulted in a sharp increase in the rate of complete oxidation of propane. Indeed, with modified catalysts, TOF increased up to 10-fold to reach values of approximately 0.1 s^{-1} (see Table 3). It should be noted that the platinum content in these catalysts decreased.

Before addressing the most active catalysts, we will briefly consider catalysts prepared using titania, cerium, silica or aluminium fluoride, which is a strong Lewis acid.[122] These catalysts proved to be substantially more active than the catalysts prepared using alumina.[119] The Pt/TiO_2 catalyst had a higher activity due to higher adsorption capacity for propane, while Pt/CeO_2 was more active because of the additional propane oxidation pathways on the sites arranged along the perimeter of the Pt^0-Ce^{3+} system. Tungsten-promoted Pt/TiO_2 exhibited the same trends as catalysts based on alumina.[127] The introduction of WO_3 shifted the temperature dependence of conversion by 20 °C towards lower temperatures. The TOF value reached a maximum at comparable concentrations of the surface Pt^0 and Pt^{2+} species in Pt/AlF_3 (Ref. 122). The authors believe that the activation and cleavage of propane C–H bonds can take place on metallic particles and the oxidation of propane occurs on the charged Pt atoms.

For active catalysts, TOFs were indeed two orders of magnitude higher than those for Pt/Al_2O_3 (see Fig. 12 *b*). In the 1.5 – 4.5 nm range of platinum particle size, the turnover frequencies monotonically increased to reach 0.3 – 0.6 s^{-1} (see Table 3). By analogy with the action mechanism of electronegative dopants, the increase in TOF may be caused by strong interaction of platinum with an unusual support (zeolite, strontium titanate, boron nitride or silicate glass fibre). As a result, oxidized states with the Pt^0/PtO_x interface can be generated apart from metallic platinum. In the case of the Pt/USY catalyst (USY is ultratable Y zeolite), a much larger amount of propane is adsorbed at the metal/oxide interface than in the case of modified catalysts or, even more so, Pt/Al_2O_3; this is probably responsible for the high turnover frequency of this catalyst.[125] Propane adsorbed at the Pt^0/PtO_x interface can be additionally oxidized by oxygen that migrates over the surface of platinum. As for Pt/AlF_3, it was assumed that propane is activated on metallic platinum, while the oxidation of adsorbed propane takes place on PtO_x.[125] The role of 60 nm cuboid $SrTiO_3$ particles is to stabilize small (3 – 4 nm) metallic platinum particles due to their epitaxial interaction with the support.[124] During the reaction, core/shell Pt/PtO particles (Pt^0 as the core and PtO as the shell) were formed;[136] in the authors' opinion, they were responsible for the very high activity of the $Pt/SrTiO_3$ catalyst towards the oxidation of propane (TOF = 0.61 s^{-1}). When platinum is deposited on alumina or $SrTiO_3$ powder, the platinum particles of approximately the same size were oxidized almost completely under the reaction conditions, so that the turnover frequency decreased by more than two orders of magnitude.[124]

The TOF value for the oxidation of propane with the Pt/h-BN catalyst was somewhat lower (see Table 3). Considering the established correlation between the turnover frequency and the concentration of surface Pt^0 atoms, the authors concluded that the active species are 2 nm metallic platinum particles stabilized at the integrain boundaries of hexagonal boron nitride.[126] Unlike highly dispersed platinum particles supported on alumina, they were easily reduced, which ensured high activity of the Pt/h-BN catalyst. However, apart from metallic platinum, there remained a noticeable amount of oxidized Pt^{2+} species, which might also participate in the propane oxidation.

Participation of charged platinum species in the oxidation of propane can be considered with confidence only in the case of Pt_V/GF and Pt_V/N-GF, because they were initially present in these catalysts.[40] Approximately a quater of the total amount of platinum occurred as Pt^{2+} cations, which were most likely bound to oxygen – silicon atoms (Pt–O–Si), as they were not reduced with hydrogen even at 500 °C. The TOF values were close to those for Pt/BN and were only two times lower than the TOFs for this reaction catalyzed by $Pt/SrTiO_3$ or Pt/USY. It is important that the platinum content in the glass fibre catalysts was more than an order of magnitude lower than in all group 3 catalysts (see Table 3). High activity of GF catalysts is due to the presence of Pt^0-Pt^{2+} metal oxide clusters, which are able to adsorb a large amount of propane and to activate molecular oxygen species.[40, 130] The platinum content is very low in this case, which means that two mutually exclusive problems have been solved, that is, the catalyst activity has been increased and the platinum content has been decreased.

On the basis of the results, a modified Langmuir – Hinshelwood mechanism was proposed, which includes reversible adsorption of molecular oxygen on Pt^0, irreversible propane adsorption on the Pt^0-Pt^{2+} sites followed by complete oxidation of propane by the neighbouring adsorbed oxygen molecules.[130] The kinetic model adequately describes the extremal dependences of the reaction rate over a broad range of temperatures and $O_2:C_3H_8$ ratios from 0.2 to 20 (see Fig. 11) and also unusual changes in the observed activation energy and the order of the reaction following the change in the oxygen concentration. It is worth noting that the proposed reaction mechanism is based on the concept of $Pt-PtO_x$ metal – oxide pair sites, which are able to effectively adsorb propane and activate (polarize) the C–H bond followed by the oxidation of propane by reactive molecular oxygen species. As a result, the turnover frequency increases by more than an order of magnitude in comparison with TOFs for the reaction catalyzed by platinum particles supported on alumina (see Fig. 12).

Thus, the most commonly used Pt/Al_2O_3 catalysts proved to be moderately active in the complete oxidation of propane. To increase the catalyst activity, it is necessary to increase the Pt particle size, which would inevitably increase the cost. It is more promising to dope the Pt/Al_2O_3 catalyst with vanadium and tungsten oxides and sulfates, which generate the $Pt^{\delta+}-WO_x(SO_4^{2-})$ sites. On these sites, dissociative adsorption of propane with C–H bond activation takes place, which results in a sharp increase in the reaction rate. Platinum particles efficiently interact with zeolites, $SrTiO_3$ nanoparticles and silicate GFs to form $Pt-PtO_x$ pair active sites, which ensure the highest reaction rate.

Similar conclusions can be drawn for the complete oxidation of methane catalyzed by platinum.[137–142] The effect of the O : Pt ratio in Pt/Al_2O_3 on the catalyst activity towards complete oxidation of methane was studied *in situ* by X-ray absorption near edge structure (XANES) spectroscopy.[137] It was shown that in an oxygen-free medium, the O : Pt ratio is close to 0.10, whereas in excess oxygen, it amounts to 0.16. The highest catalyst activity was observed for intermediate O : Pt ratios, that is, when platinum was partially oxidized. Similar results were obtained in a study of the size effect for Pt/Al_2O_3 catalysts. Indeed, a clear-cut TOF maximum was observed when the Pt particle size (d) was 2 nm, which corresponded to partially oxidized platinum with comparable amounts of charged and metallic platinum species.[138] When $d < 2$ nm, the state of platinum was closer to oxidized one, while for $d > 2$ nm, it was closer to the metallic state. The same trend towards increasing activity of the platinum catalyst was observed when tungsten oxide was used as the dopant.[139]

A vivid example demonstrating the key role of charged platinum species in the oxidation of methane has been reported:[140] the turnover frequency for the Pt/Cr_2O_3-catalyzed reaction was 28 times as high as the TOF for Pt/Al_2O_3. This sharp increase in the reaction rate was induced (according to XPS data) by the formation of Pt^0-Pt^{4+} dipoles at the platinum/support interface and the dissociative adsorption and subsequent oxidation of methane on these dipoles. It was assumed that these dipoles strongly polarize the C–H bond, and detachment of the first hydrogen atom occurs much more easily from adsorbed methane. The rate of complete oxidation of methane on metallic platinum sharply increased in the presence of an adjacent charged cation.[141] Similar Pt^0-PtO_x pairs were formed when the Pt/CeO_2 catalyst was promoted by sulfate anions.[142]

At the end of this Section, it is expedient to consider prospects of Pt/GF catalysts for deep oxidation of VOCs. It is obvious that an increase in the degree of dispersion of platinum particles will not increase the activity of Pt_V/GF, since in this case, the TOF values decrease (see Fig. 12 *b*). Coarsening of platinum particles confined in glass is hardly possible, since this may cause mechanical destruction of glass due to the generated stress. It seems more appropriate to introduce strong electronegative sulfates or hydrogen sulfates into the glass fibre bulk, which can considerably enhance both adsorption and polarizing capacity of metal–oxide pair sites and thus additionally increase the activity of Pt/GF catalysts.

7. Oxidative degradation of organochlorine compounds on the Pt/glass fibre catalysts

The catalysts and processes of treatment of industrial exhaust gases for the removal of organic chlorine compounds (Cl-VOCs) are subject to stringent requirements, as these compounds are highly hazardous for the environment and human health.[143, 144] First of all, this is a high catalyst activity to attain a minimum residual concentration of Cl-VOCs, which should be < 0.2 ng L^{-1} for especially toxic polychlorinated dibenzo-1,4-dioxins.[145] Second, the catalysts should be stable against the action of the reaction product, hydrogen chloride, moreover, in the presence of water vapour. Finally, the catalyst selectivities to CO_2 and HCl should approach 100%, that is, in order to avoid the formation of more hazardous secondary products such as phosgene or dioxins, no carbon monoxide or molecular chlorine should be formed during combustion of Cl-VOCs.

The catalysts used include transition metal oxides or oxide mixtures[146–156] and H-forms of highly acidic zeolites.[157–160] However, these catalysts are insufficiently selective due to the formation of carbon monoxide and molecular chlorine, and zeolites can be carbonized due to low oxidative capacity. In addition, hydrogen chloride and chlorine can promote catalyst deactivation due to the leaching of active transition metal cations. The supported catalysts containing platinum group metals proved to be most efficient in the oxidative destruction of Cl-VOCs,[161–168] although they were also deactivated during the reaction.[169] Therefore, attempts to test platinum catalysts based on glass fibre materials in the oxidative degradation of chlorinated organic compounds were of considerable interest.[170] It should be noted that the authors did not carry out detailed kinetic study, as in the case of combustion of organic compounds (see the previous Section), since the main goal was to completely degrade Cl-VOCs to safe CO_2, H_2O and HCl. In addition, it was very important to minimize the residual concentration of organochlorine compounds and CO and completely suppress the formation of highly hazardous molecular chlorine, phosgene, furans and dioxins. Low concentrations were analyzed using a highly sensitive IR analyzer with a gas cell with an optical path length of 4 m. This allowed determination of the above compounds in concentrations of $< 0.1-1$ ppm.

From the data presented in Table 4, it can be seen that the Pt_V/GF catalyst showed high activity in the combustion of monochlorinated benzene and n-butane and disubstituted 1,2-dichloroethane.

A virtually complete conversion of Cl-VOCs was attained at moderate temperatures, 400–450 °C. The catalyst showed an almost 100% selectivity, *i.e.*, the destruction did not give hazardous products such as carbon monoxide, molecular chlorine or phosgene. The catalyst contained 0.02% of platinum and was prepared using Al silicate glass fibres possessing high Brønsted acidity.[45, 46] Apparently, the key step is elimination of a chlorine atom from the Cl-VOC molecule to give the corresponding carbenium cation, which is readily oxidized to complete oxidation products. There is an analogy with complete oxidation of toluene catalyzed by 0.2% Pt/SBA-15,[108] in which C–C bond cleavage took place on low-coordinate platinum

Table 4. Characteristics of the oxidative destruction of Cl-VOCs with air catalyzed by 0.02% Pt_V/GF.[170]

Cl-VOC	Content of Cl-VOC (%)	Space velocity /h^{-1}	Temperature of 100% conversion /°C	Residual concentration /ppm
Chlorobenzene	1.3	12 000	400	< 1
1-Chlorobutane	0.5	12 000	450	< 1
$C_2H_4Cl_2$ + 3% C_3H_8	0.5	20 400	500	40
$C_2H_4Cl_2$ + 2% H_2O	0.5	19 300	450	10
$C_2H_4Cl_2$ + 3% C_3H_8 + 2% H_2O	0.6	16 800	400	< 1

atoms to give phenyl and methyl intermediates, which were readily oxidized with oxygen to CO_2 and H_2O. In the absence of oxygen, thee carbenium cation can be deprotonated to the corresponding alkene.[171] Indeed, heating of the catalyst in an inert gas at 400 °C induced an almost quantitative dehydrochlorination of n-butyl chloride to but-1-ene with a selectivity of 96%.

The oxidation of 1,2-dichloroethane containing two chlorine atoms was significantly retarded compared to the degradation of monosubstituted organochlorine compounds, and complete conversion was not attained upon temperature rise up to 550 °C. It is obvious that elimination of the second chlorine atom from the carbenium cation is very difficult. In addition, the process selectivity markedly decreased due to the formation of carbon monoxide, molecular chlorine, vinyl chloride and acetylene. The two last-mentioned compounds are formed, most likely, *via* side dehydrochlorination reactions of dichloroethane and vinyl chloride, respectively, and molecular chlorine is obtained in the Deacon reaction. In the dichloroethane molecule, H : Cl = 2, that is, it is equal to the limiting stoichiometry of the formation of HCl, CO_2 and H_2O. In other words, the amount of hydrogen atoms in dichloroethane is only just sufficient for the formation of hydrogen chloride; however, the formation of undesirable Cl-containing compounds would markedly decrease the selectivity to HCl. Therefore, if excess propane as an additional source of hydrogen is added to the feed gas (the propane conversion does not exceed 5% – 7%), the concentrations of dehydrochlorination products and CO substantially decreased (molecular chlorine was not detected at all), although their total content remained at the level of tens of ppm (see Table 4). If the reaction temperature further increased, the CO concentration decreased, but the concentration of the dehydrochlorination product, vinyl chloride, increased. It is noteworthy that the addition of hydrocarbons as a source of hydrogen was successfully utilized previously for the oxidative destruction of fully substituted tetrachloromethane [172] and perchloroethylene.[167]

The catalytic degradation of dichloro-substituted alkanes, in particular, dichloromethane proceeded most fully in the presence of water vapour.[168, 173] In this case, the oxidation occurred by a bifunctional mechanism with participation of the support (alumina).[168] First, hydrolysis of the C – Cl bond takes place, resulting in evolution of HCl and formation of hydroxymethoxyl intermediates (formaldehyde precursors), which are then oxidized by oxygen chemisorbed on platinum.[168] The role of water was to regenerate the hydroxyl groups on alumina. Indeed, the addition of 2% H_2O to the reaction mixture sharply increased the rate of oxidative degradation of dichloroethane, so that complete conversion took place at 450 °C, with the residual CO concentration being not higher than 10 ppm (see Table 4). Finally, upon simultaneous addition of propane and water, the residual concentrations of all hazardous compounds decreased below the sensitivity level of IR analysis (< 1 ppm), which was observed for the degradation of chlorobenzene and butyl chloride. As distinct from supported catalysts based on noble metals or mixed transition metal oxides, the Pt_V/GF catalyst demonstrated good stability for at least 100 h of testing in the oxidative degradation of dichloroethane.

Of most interest was the testing of the Pt_V/GF catalyst in the oxidative degradation of polychlorinated dibenzo-1,4-dioxins, which are most stable and hazardous compounds. Supported Pt catalysts are less active towards the degradation of dioxins than the supported oxide catalysts $VO_x - CeO_2/TiO_2$ (Ref. 145) and $V_2O_5 - WO_3/TiO_2$ (Ref. 174). A glass fibre catalyst containing 0.01% platinum was tested in a certified laboratory of the Environmental Protection Agency in Durham (USA).[114] As the test dioxin, the least degradable 1,2,3,4-tetrachlorodibenzo-1,4-dioxin (1,2,3,4-TeCDD) was chosen; the 1,2,3,4-TeCDD molecule represents two benzene rings connected by two bridging (ether) oxygen atoms, with all four hydrogen atoms in one ring being replaced by chlorine. In the presence of Pt_V/GF, the degree of degradation of 1,2,3,4-TeCDD was 95%, which corresponded to the residual dioxin concentration of < 0.1 ng L^{-1} (0.4 ppb).[114] It is noteworthy that no secondary reaction products with equal toxicity were formed during testing.

8. Conclusion

Studies of the molecular structure and viscosity of silicate glass fibre materials and diffusion of gas molecules showed that, in terms of its characteristics, glass more closely resembles a liquid rather than a solid. The key properties that make glass fibres quite attractive for the use in catalysis were identified. First, this is the ability of glass to confine highly dispersed palladium and platinum particles of 1 – 2 nm size at a 10 nm depth in the bulk of glass fibres. Therefore, despite the extremely low content of the metal (0.01% – 0.02%), GF catalysts showed high activities in the selective hydrogenation of acetylene and complete oxidation of hydrocarbons. These catalysts are not sintered during the reaction or during the high-temperature annealing up to 800 °C; they are not prone to undergo restructuring of metal particles or changes in the chemical composition. The high mobility of reactants in glass ensures their unhindered and fast transfer to active sites and, hence, the catalytic reaction is not diffusion-limited.

The turnover frequency for the selective hydrogenation of acetylene depends little on the nature of the support or the degree of dispersion of palladium particles. Therefore, the reaction is structure-insensitive, with the rate-limiting step being the hydrogen atom addition to an adsorbed acetylene molecule. However, the TOF values markedly decrease on going to single palladium atoms, which is most likely due to a change in the reaction mechanism. Indeed, recently it was shown [97] that hydrogen and propylene are adsorbed on a platinum atom, and then the alkene is hydrogenated first to the isopropyl intermediate and then to propane.

An important feature is the ability of glass fibres to selectively absorb (dissolve) polar and easily polarizable molecules such as acetylene, but not ethylene or ethane. Therefore, ethylene present in the gas phase is not involved in hydrogenation, and the selectivity of Pd_V/GF remains high until acetylene is completely converted. This actually suppressed the undesirable reaction pathway, that is, hydrogenation of gas-phase ethylene to ethane, which decreases the selectivity as approaching 100% conversion of acetylene. Nevertheless, ~40% of acetylene is still converted to ethane rather than desorbed as ethylene because of relatively large size of Pd_V particles (1 – 2 nm). High selectivity is inherent in single palladium atoms; however, this advantage is cancelled out by their low activity.

The activity and selectivity are more balanced for bimetallic catalysts with isolated palladium atoms. How-

ever, during the reaction, segregation of the alloy surface apparently takes place to give palladium clusters, which increases the reaction rate, but decreases the selectivity because of the increase in the binding energy between ethylene and palladium. In this respect, glass fibre catalysts are more promising; it is only necessary to decrease the degree of dispersion of palladium or maintain palladium in the oxidized state by means of doping with electronegative sulfates.

The TOF values of the catalyst for complete oxidation of propane decrease almost linearly with the degree of dispersion of platinum, *i.e.*, the reaction is structure-sensitive. The turnover frequency of the Pd_V/N-GF catalyst is 1–2 orders of magnitude higher than that of Pt/Al_2O_3 for the same reaction. This is attributable to the formation of $Pt^{2+}-Pt^0$ mixed metal–oxide sites, which enhances the propane adsorption and leads to a much higher rate of the complete oxidation of propane. Similar activities were shown for Pt particles deposited on zeolites or nanocuboid $SrTiO_3$, which is attributable to the strong interaction of platinum with the support, resulting in generation of PtO_x active states, able to efficiently oxidize adsorbed propane. A modified Langmuir–Hinshelwood mechanism is proposed, which includes reversible adsorption of molecular oxygen on Pt^0, irreversible adsorption of propane on $Pt^{2+}-Pt^0$ sites and its subsequent oxidation by neighbouring oxygen molecules. The kinetic model describes well the extremal dependences of the reaction rate over broad temperature and $O_2:C_3H_8$ ranges and also unusual kinetic features such as changes in the activation energy and order of reaction with increasing oxygen concentration.

High activity and selectivity were found for the Pt_V/GF catalyst in the oxidative degradation of chlorinated organic compounds. The residual concentration did not exceed 0.1–1 ppm and the process was not accompanied by the formation of hazardous secondary products (chlorine, phosgene, furans). Difficult-to-degrade Cl-VOCs were oxidized only in the presence of water vapour (hydrolysis of the C–Cl bond) and propane as a source of hydrogen. Under relatively mild conditions, the GF catalyst provided an approximately 95% degradation of 1,2,3,4-tetrachlorodibenzodioxin.

High activity and stability of the Pt_V/GF catalyst were confirmed in detoxification of organic compounds in the exhaust gases of the isoprene plant Monomer (Nizhnekamskneftekhim company).[175] The catalyst was loaded into the exhaust gas combustion reactor with a capacity of 15 000 $m^3\ h^{-1}$. In order to avoid non-uniformity across the reactor, the catalyst bed was structured: it consisted of 66 spiral type cartridges, representing alternating layers of glass fabric (catalyst) and a 3D metallic Rabitz wire lattice.[175] The metallic mesh served as a sort of framework. The total amount of the catalyst was ~1000 kg and the platinum content in the catalyst was 0.02 mass %, which is only 200 g. For safety, the gas flow was highly diluted with water vapour (up to 70%–80%), so that the oxygen concentration decreased to 5%. The gas temperature at the inlet of the reactor varied from 270 to 340 °C. The VOC concentration in exhaust gases was highly variable. Therefore, we present the average values, mg m^{-3}: carbon monoxide, 4000; isoprene, 700; isobutylene, 750; formaldehyde, 20; and dimethyldioxane, 5. During continuous operation for five years, the degree of gas purification was 99.6%–99.8%; thus, the residual content of hazardous organic compounds was much lower than the maximum allowable concentrations.

The second batch was processed with a better catalyst based on Zr silicate glass fabric. Measurements of the purified gas composition performed at intervals for more than six years showed that the concentration of residual gases did not exceed 1 ppm, *i.e.*, it was at the sensitivity level of gas chromatographic analysis.

The results convincingly demonstrate high activity of the Pt_V/GF catalyst, and, which is most important, high operation stability of the catalyst under very unfavourable conditions. It is noteworthy that under these conditions, the copper chromium oxide catalyst IKT-12-8 was deactivated after only several months of operation. The stability of glass fibre catalysts to deactivation is due to three main reasons. First, glass fibres are non-porous. Meanwhile, pores can be easily plugged by, for example, carbon deposits or dust. Second, platinum or palladium clusters confined in the glass fibre bulk are not sintered even at very high temperatures, as they are chemically bound to the silicate matrix. Finally, the active sites are confined in the glass, *i.e.*, they do not directly contact with catalytic poisons, in particular, with submicrometre phosphorus oxide particles that enter the catalyst bed with the gas flow.

Figures 7 and 11 are courtesy of Elsevier; Figures 1–6, 8, 12 were compiled by the author of the review using data from published sources, which are referred to as in the Figure captions.

The author is sincerely grateful to E.A.Paukshtis, E.V.Kovalev, A.P.Suknev and Yu.K.Gulyaeva for the help in conducting experiments and useful discussion.

The review was prepared within the framework of the state assignment for the Institute of Catalysis, Siberian Branch, Russian Academy of Sciences (Project AAAA-A17-117041710083-5).

References

1. M.Jacoby. *Chem. Eng. News*, **90** (25), 34 (2012)
2. Yu.Matatov-Meytal, M.Sheintuch. *Appl. Catal., A*, **231**, 1 (2002)
3. E.Reichelt, M.P.Heddrich, A.Michaelis. *Appl. Catal., A*, **476**, 78 (2014)
4. V.V.Barelko, M.V.Kuznetsov, V.G.Dorokhov, I.Parkin. *Russ. J. Phys. Chem.*, **11**, 606 (2017)
5. D.M.Nicholas, Y.T.Shah, I.A.Zlochower. *Ind. Eng. Chem. Prod. Res. Dev.*, **15**, 29 (1976)
6. D.M.Nicholas, Y.T.Shah. *Ind. Eng. Chem. Prod. Res. Dev.*, **15**, 35 (1976)
7. A.Inayat, B.Reinhardt, J.Herwig, Ch.Kuster, H.Uhlig, Sh.Krenkel, E.Raedleind, D.Enke. *New J. Chem.*, **40**, 4095 (2016)
8. B.Zhu, Z.Zhang, Y.Wu, J.Zhang, Z.Imran, D.Zhang. *J. Shanghai Jiao Tong Univ. (Sci.)*, **24**, 681 (2019)
9. J.Kullmann, D.Enke, S.Thränert, R.Krause-Rehberg, A.Inayat. *Colloids Surf., A*, **357**, 17 (2010)
10. T.Titze, C.Chmelik, J.Kullmann, L.Prager, E.Miersemann, R.Gläser, D.Enke, J.Weitkamp, J.Kärger. *Angew. Chem., Int. Ed.*, **54**, 5060 (2015)
11. T.Yazawa, F.Machida, N.Kubo, T.Jin. *Ceram. Int.*, **35**, 3321 (2009)
12. Z.Liu, P.Fang, S.Wang, Y.Gao, F.Chen, F.Zheng, Y.Liu, Y.Dai. *J. Mol. Catal., A*, **363–364**, 159 (2012)
13. J.Palau, M.Colower, J.Penya-Roja, V.Martinez-Soria. *Ind. Eng. Chem. Res.*, **51**, 5986 (2012)
14. N.Hashim, P.Natarajan, A.K.Ray. *Ind. Eng. Chem. Res.*, **53**, 18637 (2014)

15. C.Passalía, E.Nocetti, O.Alfano, R.Brandi. *Environ. Sci. Pollut. Res.*, **24**, 6382 (2017)
16. M.Tasbihi, I.Calin, A.Šuligoja, M.Fanettic, U.L.Štangara. *J. Photochem. Photobiol., A*, **336**, 89 (2017)
17. A.J.Jafari, R.R.Kalantary, A.Esrafili, H.Arfaeinia. *Proc. Safety Environ. Protect.*, **116**, 377 (2018)
18. A.J.Jafari, H.Arfaeinia, B.Ramavandi, R.R.Kalantary, A.Esrafily. *Air Qual. Atmos. Health*, **12**, 1181 (2019)
19. L.Kiwi-Minsker, I.Yuranov, E.Slavinskaøa, V.Zaikovskii, A.Renken. *Catal. Today*, **59**, 61 (2000)
20. A.S.Brichkov, A.N.Shamsutdinova, O.S.Khalipova, A.O.Rogacheva, T.V.Larina, T.S.Glazneva, S.V.Cherepanova, E.A.Paukshtis, A.A.Buzaev, V.V.Kozik, Y.-W.Chen. *J. Chem. Technol. Biotechnol.*, **94**, 3618 (2019)
21. A.N.Shamsutdinova, A.S.Brichkov, E.A.Paukshtis, T.V.Larina, S.V.Cherepanova, T.S.Glazneva, V.V.Kozik. *Catal. Commun.*, **89**, 64 (2017)
22. L.G.Simonova, V.V.Barelko, A.V.Toktarev, A.F.Cherashov, V.A.Chumachenko, B.S.Bal'zhinimaev. *Kinet. Catal.*, **43**, 61 (2002)
23. B.S.Bal'zhinimaev, L.G.Simonova, V.V.Barelko, A.V.Toktarev, V.I.Zaikovskii, V.A.Chumachenko. *Chem. Eng. J.*, **91**, 181 (2003)
24. V.V.Barelko, A.P.Khrushch, A.F.Cherashev, I.A.Yuranov, V.A.Matyshak, O.N.Sil'chenkova, T.I.Khomenko, O.V.Krylov. *Kinet. Catal.*, **41**, 655 (2000)
25. I.Yuranov, L.Kiwi-Minsker, M.Slin'ko, E.Kurkina, E.Tolstunova, A.Renken. *Chem. Eng. Sci.*, **55**, 2827 (2000)
26. Ch.Krauns, V.Barelko, G.Fabre, J.Tredicce, V.Krinsky. *Catal. Lett.*, **72** 161 (2000)
27. K.Donadel, C.Rambo, W.Chacon, M.Innocentini, R.Catupan, D.Muller, A.Oliveira. *Ceram. Int.*, **38** 6243 (2012)
28. T.A.Balandina, T.Yu.Larina, N.I.Kuznetsova, B.S.Bal'zhinimaev. *Kinet. Catal.*, **49**, 499 (2008)
29. J.Medina-Valtierra, C.Frausto-Reyes, G.Camarillo-Martinez, J.A.Ramírez-Ortiz. *Appl. Catal., A*, **56**, 36 (2009)
30. I.V.Desyatykh, A.A.Vedyagin, I.V.Mishakov, Yu.V.Shubin. *Appl. Surf. Sci.*, **349**, 21 (2015)
31. V.G.Dorokhov, V.V.Barelko, L.A.Bykov, R.A.Basimova, M.L.Pavlov, A.V.Askarova. *Dokl. Chem.*, **438**, 148 (2011)
32. V.Holler, D.I.Wegricht, I.Yuranov, L.Kiwi-Minsker, A.Renken. *Chem. Eng. Technol.*, **23**, 251 (2000)
33. Y.X.Zhang, X.L.Guo, M.Huang, X.D.Hao, Y.Yuan, C.Hua. *J. Phys. Chem. Solids*, **83**, 40 (2015)
34. Yu.Matatov-Meytal, V.V.Barelko, I.Yuranov, L.Kiwi-Minsker, A.Renken, M.Sheintuch. *Appl. Catal., B*, 31233 (2001)
35. H.T.Yang, Zh.P.Fang, X.Y.Fu, L.F.Tong. *Catal. Commun.*, **9**, 1092 (2008)
36. A.Elhage, B.Wang, N.Marina, M.L.Marin, M.Cruz, A.E.Lanterna, J.C.Scaiano. *Chem. Sci.*, **9**, 6844 (2018)
37. B.S.Bal'zhinimaev, E.M.Sadovskaya, A.P.Suknev. *Chem. Eng. J.*, **154**, 2 (2009)
38. B.S.Bal'zhinimaev, V.V.Barelko, A.P.Suknev, E.A.Paukshtis, L.G.Simonova, V.B.Goncharov, V.L.Kirillov, A.V.Toktarev. *Kinet. Catal.*, **43**, 542 (2002)
39. B.S.Bal'zhinimaev, E.V.Kovalyov, A.P.Suknev, E.A.Paukshtis, D.F.Khabibulin, I.S.Batueva, A.N.Salanov, M.G.Riley. *Ind. Eng. Chem. Res.*, **56**, 10318 (2017)
40. B.S.Bal'zhinimaev, E.V.Kovalyov, V.V.Kaichev, A.P.Suknev, V.I.Zaikovskii. *Top. Catal.*, **60**, 73 (2017)
41. Yu.K.Gulyaeva, V.V.Kaichev, V.I.Zaikovskii, E.V.Kovalyov, A.P.Suknev, B.S.Bal'zhinimaev. *Catal. Today*, **245**, 139 (2015)
42. D.Hülsenberg, A.Harnisch, A.Bismarck. In *Microstructuring of Glasses*: *Silicate Glasses: a Class of Amorphous Materials*. Vol. 87. (Eds R.Hull, R.M.Osgood, J.Parisi, H.Warlimont). (Berlin, Heidelberg: Springer, 2008). P. 56
43. G.N.Greaves. *J. Non-Cryst. Solids*, **71**, 203 (1985)
44. L.G.Simonova, V.V.Barelko, O.B.Lapina, E.A.Paukshtis, V.V.Terskikh, V.I.Zaikovskii, B.S.Bal'zhinimaev. *Kinet. Catal.*, **42**, 693 (2001)
45. T.S.Glazneva, V.P.Shmachkova, L.G.Simonova, E.A.Paukshtis. *React. Kinet. Catal. Lett.*, **92**, 303 (2007)
46. T.S.Glazneva, E.M.Sadovskaya, A.P.Suknev, V.B.Goncharov, L.G.Simonova, E.A.Paukshtis, B.S.Bal'zhinimaev. *Appl. Catal., A*, **366**, 262 (2009)
47. B.S.Bal'zhinimaev, E.A.Paukshtis, O.B.Lapina, A.P.Suknev, V.L.Kirillov, P.E.Mikenin, A.N.Zagoruiko. *Stud. Surf. Sci. Catal.*, **175**,43 (2010)
48. O.B.Lapina, D.F.Khabibulin, V.V.Terskikh. *Solid State Nucl. Magn. Reson.*, **39**, 47 (2011)
49. O.B.Lapina, D.F.Khabibulin, E.S.Papulovskiy, A.A.Shubin, Yu.K.Gulyaeva. *J. Struct. Chem.*, **54**, S152 (2013)
50. Yu.K.Gulyaeva, A.P.Suknev, E.A.Paukshtis, B.S.Bal'zhinimaev. *J. Non-Cryst. Solids*, **357**,3338 (2011)
51. B.C.Bunker. *J. Non-Cryst. Solids*, **179**, 300 (1994)
52. W.J.Malfait, X.Xue. *Geochim. Cosmochim. Acta*, **74**, 719 (2010)
53. R.Hellmann, S.Cotte, E.Cadel, S.Malladi, L.S.Karlsson, S.Lozano-Perez, M.Cabie, A. Seyeux. *Nat. Mater.*, **14**, 307 (2015)
54. B.S.Bal'zhinimaev. In *Advances in Materials Science Research*. Vol. 36. (Ed. M.C.Wythers). (New York: Nova Science Publishers, 2019). P. 1
55. T.S.Glazneva, E.A.Paukshtis, E.M.Sadovskaya,T.V.Larina, B.S.Bal'zhinimaev. *J. Am. Ceram. Soc.*, **102**, 5164 (2019)
56. E.M.Sadovskaya, A.P.Suknev, A.V.Toktarev, L.G.Simonova, E.A.Paukshtis, B.S.Bal'zhinimaev. *Kinet. Catal.*, **47**, 131 (2006)
57. J.E.Shelby. *J. Am. Ceram. Soc.*, **91**, 703 (2008)
58. C.Mansas, J.-M.Delaye, T.Charpentier, F.Bruguier, O.Bouty, B.Penelon, H.Arena, D.Rébiscoul. *J. Phys. Chem. C*, **121**, 16201 (2017)
59. G.S.Frankel, J.D.Vienna, J.Lian, J.R.Scully, S.Gin, J.V.Ryan, J.Wang, S.H.Kim, W.Windl, J.Du. *Mater. Degradat.*, **2**, 15 (2018)
60. B.S.Bal'zhinimaev, E.A.Paukshtis, E.V.Kovalyov. *Catal. Ind.*, **12**, 56 (2020)
61. J.C.D.Brand, A.I.Scott. In *Elucidation of Structures by Physical and Chemical Methods*. Vol. XI. Pt. 1. (Ed. K.W.Bentley). (New York, London: Wiley, 1963). P. 61
62. A.Sarcany, L.Guczi, A.N.Weiss. *Appl. Catal.*, **10**,369 (1984)
63. X.Ma, X.Wang, C.Song. *J. Am. Chem. Soc.*, **131**, 5777 (2009)
64. Q.Chen, F.Fan, D.Long, X.Liu, X.Liang, W.Qiao, L.Ling. *Ind. Eng. Chem. Res.*, **49**, 11408 (2010)
65. S.Gin, M.Collin, P.Jollivet, M.Fournier, Y.Minet, L.Dupuy, T.Mahadevan, S.Kerisit, J.Du. *Nat. Commun.*, **9**, 2169 (2018)
66. C.Cailleteau, F.Angeli, F.Devreux, S.Gin, J.Jestin. P.Jollivet, O.Spalla. *Nat. Mater.*, **7**, 978 (2008)
67. M.Tribet, A.H.Mir, C.Gillet, C.Jegou, S.Mougnaud, J.A.Hinks, S.E.Donnelly, S.Peuget. *J. Phys. Chem. C*, **124**, 10032 (2020)
68. E.A.Paukshtis. *Stud. Surf. Sci. Catal.*, **130**, 3231 (2000)
69. B.S.Bal'zhinimaev, A.P.Suknev, Yu.K.Gulyaeva, E.V.Kovalyov. *Catal. Ind.*, **7**, 267 (2015)
70. Yu.K.Gulyaeva, V.V.Kaichev, V.I.Zaikovskii, A.P.Suknev, B.S.Bal'zhinimaev. *Appl. Catal., A*, **506**, 197 (2015)
71. B.S.Bal'zhinimaev, V.N.Parmon. *Top. Catal.*, **55**, 1289 (2012)
72. V.V.Malakhov, I.G.Vasil'eva. *Russ. Chem. Rev.*, **77**, 370 (2008)
73. L.S.Dovlitova, A.A.Pochtar', V.V.Malakhov. *J. Anal. Chem.*, **68**, 72 (2013)
74. A.Borodziński, G.C.Bond. *Catal. Rev.*, **48**, 91 (2006)
75. A.Borodziński, G.C.Bond. *Catal. Rev. Sci. Eng.*, **50**, 379 (2008)
76. A.Pachulski, R.Schödel, P.Claus. *Appl. Catal., A*, **400**, 14 (2011)

77. I.S.Mashkovskii, O.P.Tkachenko, G.N.Baeva, A.Yu.Stakheev. *Kinet. Catal.*, **50**, 768 (2009)
78. G.X.Pei, X.Y.Liu, A.Wang, A.F.Lee, M.A.Isaacs, L.Li, X.Pan, X.Yang, X.Wang, Zh.Tai, K.Wilson, T.Zhang. *ACS Catal.*, **5**, 3717 (2015)
79. Y.Zhang, W.Diao, C.T.Williams, J.R.Monnier. *Appl. Catal., A*, **469**, 419 (2014)
80. X.Huang, H.Yan, L.Huang, X.Zhang, Y.Lin, J.Li, Y.Xia, Y.Ma, Zh.Sun, Sh.Wei, J.Lu. *J. Phys. Chem. C*, **123**, 7922 (2019)
81. F.Huang, Y.Deng, Y.Chen, X.Cai, M.Peng, Z.Jia, P.Ren, D.Xiao, X.Wen, N.Wang, H.Liu, D.Ma. *J. Am. Chem. Soc.*, **140**, 13142 (2018)
82. G.Kyriakou, M.Boucher, A.D.Jewell, E.A.Lewis, T.J.Lawton, A.E.Baber, H.L.Tierney, M.Flytzani-Stephanopoulos, E.Sykes, H.Charles. *Science*, **335**, 1209 (2012)
83. G.Giannakakis, M.Flytzani-Stephanopoulos, E.Charles, H.Sykes. *Acc. Chem. Res.*, **52**, 237 (2019)
84. J.Osswald, R.Giedigkeit, R.Gentoft, M.Armbruster, F.Girgsdies, K.Kovnir, T.Ressler, Y.Grin, R.Schlögl. *J. Catal.*, **258**, 210 (2008)
85. J.Osswald, K.Kovnir, M.Armbruster, R.Giedigkeit, R.Jentoft, U.Wild, Y.Grin, R.Schlögl. *J. Catal.*, **258**, 219 (2008)
86. D.Teschner, J.Borsodi, A.Wootsch, Z.Revay, M.Havecker, A.Knop-Gerike, S.D.Jackson, R.Schlogl. *Science*, **320**, 86 (2008)
87. D.B.Burueva, K.V.Kovtunov, A.V.Bukhtiyarov, D.A.Barskiy, I.P.Prosvirin, I. S.Mashkovsky, G.N.Baeva, V.I.Bukhtiyarov, A.Yu.Stakheev, I.V.Koptyug. *Chem. – Eur. J.*, **24**, 2547 (2018)
88. D.Duca, F.Arena, A.Parmaliana, G.Deganello. *Appl. Catal., A*, **172**, 207 (1998)
89. A.Borodziński. *Catal. Lett.*, **71**, 169 (2001)
90. A.D.Benavidez, P.D.Burton, J.L.Nogales, A.R.Jenkins, S.A.Ivanov, J.T.Miller, A.M.Karim, A.K.Datye. *Appl. Catal., A*, **482**, 108 (2014)
91. D.Mei, M.Neurock, C.M.Smith. *J. Catal.*, **268**, 181 (2009)
92. G.Bond. *Metal-Catalysed Reactions of Hydrocarbons*. (New York: Springer, 2005)
93. R.A.van Santen. *Acc. Chem. Res.*, **42**, 57 (2009)
94. W.Huang, W.Pyrz, R.F.Lobo, J.G.Chen. *Appl. Catal., A*, **333**, 254 (2007)
95. R.F.Hicks, A.T.Bell. *J. Catal.*, **205**, 205 (1984)
96. A.S.Crampton, M.D.Rötzer, C.J.Ridge, F.F.Schweinberger, U.Heiz, B.Yoon,U.Landman. *Nat. Commun.*, **7**, 10389 (2016)
97. B.Zhang, G.Sun, S.Ding, H.Asakura, J.Zhang, P.Sautet, N.Yan. *J. Am. Chem. Soc.*, **141**, 8185 (2019)
98. M.A.Esteruelas, L.A.Oro. *Chem. Rev.*, **98**, 577 (1998)
99. O.G.Salnikov, D.A.Barskiy, D.B.Burueva, Yu.K.Gulyaeva, B.S.Balzhinimaev, K.V.Kovtunov, I.V.Koptyug. *Appl. Magn. Reson.*, **45**, 1051 (2014)
100. J.H.Kang, E.W.Shin, W.J.Kim, J.D.Park, S.H.Moon. *Catal. Today*, **63**, 183 (2000)
101. Q.Zhang, L.Li, X.Liu, Q.Zhu. *Appl. Catal., A*, **197**, 221 (2000)
102. S.K.Kim, J.H.Lee, I.Y.Ahn, W.J.Kim, S.H.Moon. *Appl. Catal., A*, **401**, 12 (2011)
103. J.Feng, X.Ma, Y.He, D.G.Evans, D.Li. *Appl. Catal., A*, **413**, 10 (2012)
104. S.Leviness, A.H.Weiss, Z.Schay, L.Guczi. *J. Mol. Catal.*, **25**, 131 (1984)
105. C.Ledesma, J.Yang, D.Chen, A.Holmen. *ACS Catal.*, **4**, 4527 (2014)
106. L.Liu, D.M.Meira, R.Arenal, P.Concepcion, A.V.Puga, A.Corma. *ACS Catal.*, **9**, 10626 (2019)
107. M.A.Spronsen, K.Daunmu, C.R.O'Connor, T.Egle, H.Kersell, J.Oliver-Meseguer, M.B.Salmeron, R.J.Madix, P.Sautet, C.M.Friend. *J. Phys. Chem. C*, **123**, 8312 (2019)
108. E.Vignola, S.N.Steinmann, B.D.Vandegehuchte, D.Curulla, P.Sautet. *J. Phys. Chem. C*, **120**, 26320 (2016)
109. D.Stacchiola, F.Calaza, T.Zheng, W.T.Tysoe. *J. Mol. Catal. A: Chem.*, **228**, 35 (2005)
110. S.Ojala, S.Pitkaaho, T.Laitinen, N.N.Koivikko, R.Brahmi, J.Gaalova, L.Matejova, A.Kucherov, S.Paivarinta, C.Hirschmann, T.Nevanpera, M.Riihimaki, M.Pirila, R.L.Keiski. *Top. Catal.*, **54**, 1224 (2011)
111. L.F.Liotta. *Appl. Catal., B*, **100**, 403 (2010)
112. M.Garcia-Dieguez, Y.-H.(C).Chin, E.Iglesia. *J. Catal.*, **285**, 260 (2012)
113. Y.T.Lai, T.C.Chen, Y.K.Lan, B.S.Chen, J.H.You, Ch.M.Yang, N.C.Lai, J.H.Wu, Ch.S.Chen. *ACS Catal.*, **4**, 3824 (2014)
114. A.P.Suknev, Yu.K.Gulayeva, E.V.Kovalyov, V.I.Zaikovskii, B.S.Bal'zhinimaev. In *Proceedings of the 247th ACS National Meeting and Exposition*. (Washington,DC: American Chemical Society, 2014). P. 74
115. H.Yoshida, Y.Yazawa, T.Hattori. *Catal. Today*, **87**, 19 (2003)
116. G.Corro, J.L.G.Fierro, V.C.Odilon. *Catal. Commun.*, **4**, 371 (2003)
117. A.M.Gololobov, I. E.Beck, G.O.Bragina, V.I.Zaikovskii, A.B.Ayupov, N.S.Telegina, V.I.Bukhtiyarov, A.Yu.Stakheev. *Kinet. Catal.*, **50**, 830 (2009)
118. X.Wu, L.Zhang, D.Weng, S.Liu, Z.Si, J.Fan. *J. Hazard. Mater.*, **225**, 146 (2012)
119. M.S.Avila, C.I.Vignatti, C.R.Apesteguía, T.F.Garetto. *Chem. Eng. J.*, **241**, 52 (2014)
120. C.P.O'Brien, G.R.Jenness, H.Dong, D.G.Vlachos, I.C.Lee. *J. Catal.*, **337**, 122 (2016)
121. A.Tomita, T.Miki, Y.Tai. *Appl. Catal., A*, **522**, 138 (2016)
122. X.Li, Y.-R.Liu, W.-M.Liao, A.-P.Jia, Y.-J.Wang, J.-Q.Lu, M.-F.Luo. *Appl. Surf. Sci.*, **475**, 524 (2019)
123. W.M.Liao, Y.R.Liu, P.P.Zhao, B.H.Cen, C.Tang, A.P.Jia, J.Q.Lu. *Appl. Catal., A*, **590**, 117337 (2020)
124. J.A.Enterkin, W.Setthapun, J.W.Elam, S.T.Christenesen, F.A.Rabuffetti, L.D.Marks, P.C.Stair, K.R.Poeppelmeier, C.L.Marshall. *ACS Catal.*, **1**, 629 (2011)
125. H.Luo, X.-D.Wu, D.Weng, S.Liu, R.Ran. *Rare Met.*, **36**, 1 (2017)
126. Y.-R.Liu, X.Li, W.-M.Liao, A.-P.Jia, Y.-J.Wang, M.-F.Luo, J.Q.Lu. *ACS Catal.*, **9**, 1472 (2019)
127. X.Wu, Z.Zhou, D.Weng, B.Wang. *J. Environ. Sci.*, **24**, 458 (2012)
128. Y.P.Zheng, L.H.Zhang, S.L.Wang, D.Ding, H.Zhang, M.S.Chen, H.L.Wan. *Langmuir*, **29**, 9090 (2013)
129. Y.H.Chin, C.Buda, M.Neurock, E.Iglesia. *J. Am. Chem. Soc.*, **133**, 15958 (2011)
130. E.V.Kovalyov, E.M.Sadovskaya, B.S.Bal'zhinimaev. *Chem. Eng. J.*, **349**,547 (2018)
131. S.Vajda, M.J.Pellin, J.P.Greely, C.L.Marshall, L.A.Curtiss, G.A.Ballentine, J.W.Elam, C.Catillon-Mucherie, P.C.Redfern, F.Mehmood, P.Zapol. *Nat. Mater.*, **8**, 213 (2009)
132. J.E.Park, B.B.Kim, E.D.Park. *Korean J. Chem. Eng.*, **32**, 2212 (2015)
133. L.Zhang, D.Weng, B.Wang, X.Wu. *Catal. Commun.*, **11**, 1229 (2010)
134. W.M.Liao, X.X.Fang, B.H.Cen, J.Chen, Y.R.Liu, M.F.Luo, J.Q.Lu. *Appl. Catal., B*, **272**, 118858 (2020)
135. B.Wang, X.Wu, R.Ran, Z.Si, D.Weng. *J. Mol. Catal. A: Chem.*, **356**, 100 (2012)
136. H.Wang, M.Liu, Y.Ma, K.Gong, W.Liu, R.Ran, D.Weng, X.Wu, S.Liu. *ACS Catal.*, **8**, 2796 (2018)
137. E.Becker, P.-A.Carlsson, H.Grönbeck, M.Skoglundh. *J. Catal.*, **252**, 11 (2007)
138. I.E.Beck, V.I.Bukhtiyarov, I.Yu.Pakharukov, V.I.Zaikovsky, V.V.Kriventsov, V.N.Parmon. *J. Catal.*, **268**, 60 (2009)
139. M.O'Connell, G.Kolb, R.Zapf, Y.Men, V.Vessel. *Catal. Today*, **144**, 306 (2009)

140. G.Corro, R.Torralba, U.Pal, O.Olivares-Xometl, J.L.Fierro. *J. Phys. Chem. C*, **123**, 2882 (2019)
141. X.Weng, H.Ren, M.Chen, H.Wan. *ACS Catal.*, **4**, 2598 (2014)
142. L.Kylhammar, P.-A.Carlsson, M.Skoglundh. *J. Catal.*, **284**, 50 (2011)
143. S.Pitkäaho, S.Ojala, T.Kinnunen, R.Silvonen, R.L.Keiski. *Top. Catal.*, **54**, 1257 (2011)
144. B.Huang, C.Lei, C.Wei, G.Zeng. *Environ. Int.*, **71**, 118 (2014)
145. M.Yu, W.Li, X.Lin, T.Chen, J.Yan. *Chemosphere*, **156**, 383 (2016)
146. V.Vu, J.Belkouch, A.Ould-Dris, B.Taouk. *J. Hazard. Mater.*, **169**, 758 (2009)
147. T.K.Tseng, L.Wang, C.T.Ho, H.Chu. *J. Hazard. Mater.*, **178**, 1055 (2010)
148. E.Finocchio, G.Ramis, G.A.Busca. *Catal. Today*, **169**, 3 (2011)
149. B.de Rivas, N.Guillén-Hurtado, R.Lopez-Fonseca, F.Coloma-Pascual, A.García-García, J.I.Gutiérrez-Ortiz, A.Bueno-López. *Appl. Catal., B*, **121 – 122**, 162 (2012)
150. X.Ma, X.F.He, H.Guo, L.Lv, J.Guo, H.Cao, T.Zhou. *Microporous Mesoporous Mater.*, **158**, 214 (2012)
151. L.Huang, G.Su, A.Zhang, Y.Shi, C.Xia, H.Lu, L.Li, S.Liu, M.Zheng. *J. Hazard. Mater.*, **261**, 451 (2013)
152. X.Ma, M.Zhao, Q.Pang, M.Zheng, H.Sun, J.Crittenden, Y.Zhu, Y.Chen. *Appl. Catal., A*, **522**, 70 (2016)
153. Q.Dai, L.Yin, S.Bai, W.Wang, X.Wang, X.Gong, G.Lu. *Appl. Catal., B*, **182**, 598 (2016)
154. J.Su, Y.Liu, W.Yao, Zh.Wu. *J. Phys. Chem. C*, **120**, 18046 (2016)
155. P.Yang, S.Zuo, Z.Shi, F.Tao, R.Zhou. *Appl. Catal., B*, **191**, 53 (2016)
156. A.Tang, L.Hu, X.Yang, Y.Jia, Y.Zhang. *Catal. Commun.*, **82**, 41 (2016)
157. A.Michalik-Zym, R.Dula, D.Duraczyńska, J.Kryściak-Czerwenka, T.Machej, R.P.Socha, W.Wlodarczyk, A.Gavel, J.Matusik, K.Bahranowski, E.Wisla-Walsh, L.Lityńska-Dobrzyńska, E.M.Serwicka. *Appl. Catal., B*, **174 – 175**, 293 (2015)
158. L.Intriago, E.Diaz, S.Ordóñez, A.Vega. *Microporous Mesoporous Mater.*, **91**, 161 (2006)
159. Q.Huang, X.Xue, R.Zhou. *J. Mol. Catal. A: Chem.*, **344**, 74 (2011)
160. P.Yang, S.Zuo, R.Zhou. *Chem. Eng. J.*, **323**, 160 (2017)
161. J.Giraudon, A.Elhachimi, G.Leclercq. *Appl. Catal., B*, **84**, 251 (2008)
162. S.Pitkäaho, L.Matejova, S.Ojala, J.Gaalova, R.L.Keiski. *Appl. Catal., B*, **113**, 150 (2012)
163. Q.Y.Chen, N.Li, M.F.Luo, J.Q.Lu. *Appl. Catal., B*, **127**, 159 (2012)
164. Y.Wang, H.H.Liu, S.Y.Wang, M.F.Luo, J.Q.Lu. *J. Catal.*, **311**, 314 (2014)
165. C.He, B.Xu, J.Shi, N.Qiao, Z.Hao, J.Zhao. *Fuel Proc. Technol.*, **130**, 179 (2015)
166. L.Wang, M.Sakurai, H.Kameyama. *J. Hazard. Mater.*, **15**4, 390 (2008)
167. S.Pitkäaho, S.Ojala, T.Maunula, A.Savimäki, T.Kinnunen, R.L.Keiski. *Appl. Catal., B*, **102**, 395 (2011)
168. I.Maupin, L.Pinard, J.Mijoin, P.Magnoux. *J. Catal.*, **291**, 104 (2012)
169. I.M.Freidel, A.C.Frost, K.J.Herbert, F.S.Meyer, J.C.Summers. *Catal. Today*, **17**, 367 (1993)
170. E.A.Paukshtis, L.G.Simonova, A.N.Zagoruiko, B.S.Bal'zhinimaev. *Chemosphere*, **79**, 199 (2010)
171. G.A.Olah, H.Doggweiler, J.D.Felbery, S.Frohlich, M.J.Grdina, R.Karpeles, T.Keimi, S.Inaba, W.M.Ip, K.Lammerstma, G.Salem, D.C.Tabor. *J. Am. Chem. Soc.*, **106**, 2143 (1984)
172. A.Gervasini, C.Pirola, S.Zilio, V.Ragaini. *Appl. Catal., B*, **47**, 257 (2004)
173. L.Pinard, J.Mijoin, P.Magnoux, M.Guisnet. *J. Catal.*, **215**, 234 (2003)
174. E.Finocchio, G.Busca, M.Notaro. *Appl. Catal., B*, **62**, 12 (2006)
175. A.N.Zagoruiko, S.A.Lopatin, B.S.Bal'zhinimaev, N.R.Gil'mutdinov, G.G.Sibagatullin, V.P.Pogrebtsov, I.F.Nazmieva. *Catal. Ind.*, **2**, 113 (2010)